

A very unconventional hydrocarbon play: the Mesoproterozoic Velkerri Formation of Northern Australia.

Grant M. Cox, Tectonics and Earth Systems (TES) Group, Department of Earth Sciences, The University of Adelaide, Adelaide, South Australia, Australia; grantmcox@mac.com

Alan S. Collins (corresponding author), TES Group and Mineral Exploration Cooperative Research Centre (MinEx CRC), Department of Earth Sciences, The University of Adelaide, Adelaide, South Australia, Australia; alan.collins@adelaide.edu.au

Amber J.M. Jarrett, Northern Territory Geological Survey, Darwin, Northern Territory, Australia; Amber.Jarrett@nt.gov.au

Morgan L. Blades, TES Group and Mineral Exploration Cooperative Research Centre (MinEx CRC), Department of Earth Sciences, The University of Adelaide, Adelaide, South Australia, Australia; morgan.blades@adelaide.edu.au

April V. Shannon, TES Group, Department of Earth Sciences, The University of Adelaide, Adelaide, South Australia, Australia; april.shannon@gu.se

Bo Yang, TES Group, Department of Earth Sciences, The University of Adelaide, Adelaide, South Australia, Australia; yangbo9014@gmail.com

Juraj Farkas, TES Group and MinEx CRC, Department of Earth Sciences, The University of Adelaide, Adelaide, South Australia, Australia; juraj.farkas@adelaide.edu.au

Phillip A. Hall, TES Group, Department of Earth Sciences, The University of Adelaide, Adelaide, South Australia, Australia; tony.hall@adelaide.edu.au

Brendan O'Hara, Santos Limited, Adelaide, South Australia, Australia; Brendan.O'Hara@santos.com

David Close, Santos Limited, Adelaide, South Australia, Australia; present address: Tamboran Resources, Brisbane, Queensland, Australia; David.Close@Tamboran.com

Elizabeth T. Baruch, Origin Energy Ltd., Brisbane, Queensland, Australia; Elizabeth.Baruch-Jurado@upstream.originenergy.com.au

This paper is a non-formatted pre-accepted manuscript of the paper published in AAPG Bulletin AAPG Bulletin, v. 106, no. 6 (June 2022), pp. 1213–1237. DOI:10.1306/12162120148

A very unconventional hydrocarbon play: the Mesoproterozoic Velkerri Formation of Northern Australia.

Grant M. Cox¹, Alan S. Collins^{1*}, Amber J.M. Jarrett², Morgan L. Blades¹, April V. Shannon¹, Bo Yang¹, Juraj Farkas¹, Phillip A. Hall¹, Brendan O'Hara³, David Close³, Elizabeth T. Baruch⁴

1. Tectonics and Earth Systems (TES) Group, Department of Earth Sciences, University of Adelaide, Adelaide, SA, 5005, Australia.

2. Geoscience Australia, P.O. Box 378, Canberra, ACT, 2601, Australia.

3. Santos Limited, Santos Centre, 60 Flinders Street, Adelaide, 5000, Australia.

4. Origin Energy Ltd, Level 25, 180 Ann St, Brisbane, QLD, 4000, Australia.

*Corresponding author

Abstract

The ca. 1.5–1.3 Ga Roper Group of the greater McArthur Basin is a component of one of the most extensive Precambrian hydrocarbon-bearing basins preserved in the geological record, recently assessed as containing 429 million barrels of oil and eight trillion cubic feet of gas (in place). It was deposited in an intra-cratonic sea, referred to here as the McArthur-Yanliao Gulf.

The Velkerri Formation forms the major deep-water facies of the Roper Group. Trace metal redox proxies from this formation indicate that it was deposited in stratified waters, in which a shallow oxic layer overlay suboxic to anoxic waters. These deep waters became episodically euxinic during periods of high organic carbon export. The Velkerri Formation has organic carbon contents that reach ~10 wt%. Variations in organic carbon isotopes are consistent with organic carbon enrichment being associated with increases in primary productivity and export, rather than flooding surfaces or variations in mineralogy.

Although deposition of the Velkerri Formation in an intracontinental setting has been well established, recent global reconstructions show a broader mid to low latitude gulf, with deposition of the Velkerri Formation being coeval with the widespread deposition of organic-rich rocks across northern Australia and North China. The deposition of these organic-rich

rocks may have been accompanied by significant oxygenation associated with such widespread organic carbon burial during the Mesoproterozoic.

Introduction

The greater McArthur Basin of northern Australia (Close, 2014) comprises the sedimentary fill of one of the most extensive known Precambrian hydrocarbon-bearing basins preserved in the geological record (Fig. 1). Potential source rocks have been found within the ca. 1.74 Ga McDermott and Wollgorang formations, the ca. 1.64 Ga Barney Creek Formation (and the coeval Vaughton Siltstone), the ca. 1.40–1.34 Ga Velkerri Formation and the ca. 1.34–1.31 Ga Kyalla Formation (Jackson et al., 1986; Crick et al., 1988; Page et al., 2000; Kendall et al., 2009; Cox et al., 2016; Spinks et al., 2016; Close et al., 2017; Revie, 2017; Baruch et al., 2018; Yang et al., 2018).

Petroleum exploration in the ca. 1.5 to 1.3 Ga Roper Group has continued intermittently since the first discovery of ‘live’ hydrocarbons in the Velkerri Formation in 1985 (Jackson et al., 1986). The two main targets for petroleum exploration in the Roper Group are the Velkerri Formation and the Kyalla Formation (Yang et al., 2018; Yang et al., 2019; Bodorkos et al., 2020; Yang et al., 2020), both within the Upper Roper Group (the Maiwok Subgroup; Fig. 2). The Velkerri Formation continues to generate substantial interest as an unconventional gas play (Close et al., 2017; Revie, 2017; Baruch et al., 2018); however, the Kyalla Formation also has potential as an oil and gas target (Baruch et al., 2018; Revie and Normington, 2020). Minor oil and gas shows have been identified in wells intersecting Roper Group strata (Table 1) with significant oil shows from the Jamison 1 petroleum well (Jamison sandstone reservoir), that are likely sourced from the Kyalla Formation (Lannigan and Torkington, 1991; Jarrett et al., 2019c;). Additionally, oil bleeds in Urapunga 4 are self-sourced

from the Velkerri Formation (Jackson et al., 1986). Significant gas shows in Shenandoah 1A and recent hydraulic fracturing of the Velkerri Formation in Amungee NW-1H confirmed substantial gas flows are possible (Close et al., 2017). Recent resource assessments of the Kyalla and Velkerri formations estimates an in-place resource of 429 million barrels of oil (MMbbls) and between 8 and 118 trillion cubic feet of gas (Tcf) (Revie, 2017; Schneck et al., 2019). Such estimates attest to the untapped economic potential of the Mesoproterozoic Kyalla and Velkerri formations.

In this contribution, we synthesise previous work with newly acquired data focussing principally on the biogeochemical (e.g. organic chemistry, carbon-sulfur systematics, basin redox, organic carbon isotopes) and source rock characteristics (e.g. TOC, thermal maturity) of the Velkerri Formation. Although Paleoproterozoic hydrocarbon plays in the McArthur Basin are currently in the early stages of exploration (e.g. the ca. 1.74 Ga Wollongorang Formation, and the ca. 1.64 Ga Barney Creek Formation, with its correlative, the Riversleigh Siltstone in the Mount Isa Province of Queensland), globally, the Velkerri Formation is one of the most advanced Precambrian unconventional hydrocarbon plays. Considering its Mesoproterozoic age (ca. 1.40–1.34 Ga), the Velkerri Formation offers crucial insights into Precambrian paleoenvironments that may be conducive to exploring for hydrocarbon resources of this antiquity.

Geology

The sedimentary successions of the greater McArthur Basin were subdivided by Rawlings (1999) and Close (2014) into five basin-wide, disconformity- or unconformity-bounded depositional 'packages'; in ascending stratigraphic order, the Paleoproterozoic Redbank, Goyder and Glyde packages, and the Mesoproterozoic Favenc and Wilton packages.

Each package is characterised by similarities in age, stratigraphic position, lithofacies composition, style and composition of volcanism, and basin-fill geometry. The Roper Group (Fig. 2) represents the Wilton package in the southern McArthur Basin and covers over ~145 000 km² of northern Australia in either surface outcrop or the sub-surface (Jackson et al., 1986; Abbott and Sweet, 2000; Munson, 2016). Significant lateral thickness changes occur within the Roper Group, it is thinnest (<500 m) over the north–south trending Batten Fault Zone, ~1–2 km thick in the vicinity of the Urapunga Fault Zone and thickens dramatically to >5km south of the Urapunga Fault Zone in the eastern Beetaloo Sub-basin (Plumb and Roberts, 1992; Abbott and Sweet, 2000; Rawlings et al., 2004; Munson, 2016; Williams, 2019)(Fig. 1). This has been interpreted to represent the main depocentre of the Roper Group (Plumb and Wellman, 1987; Abbott and Sweet, 2000; Williams, 2019).

Recent palaeomagnetic-based reconstructions (Collins et al., 2019; Cawood et al., 2020) place the North Australian Craton in mid to low latitudes at ca. 1.3 Ga, plausibly juxtaposed against Laurentia (North America), Siberia, South China and the North China Craton (Fig. 3). Collins et al. (2019) suggested that the broader marine environment formed a large gulf, hereafter referred to as the McArthur-Yanliao Gulf. Both the McArthur Basin and the Yanliao Basin (North China Craton) preserve coeval black shales. The black shales of the Velkerri Formation (northern Australia) are constrained by a combination of absolute ages (Re–Os) and maximum depositional ages (U–Pb detrital zircons) to be between 1.39 ± 0.01 Ga (2σ) and 1.36 ± 0.02 Ga (2σ) (Bodorkos et al., 2020; Kendall et al., 2009; Yang et al., 2018). The black shales of the Xiamaling Formation, within the North China Craton, were deposited at 1.38 ± 0.01 Ga (Zhang et al., 2015; Zhang et al., 2017), and have comparable TOC levels to that of the Velkerri Formation.

The Velkerri Formation is the initial relatively deep-water facies of a shoaling upward sequence (the interpreted Veloak Sequence of Abbott and Sweet, 2000), which comprises the dominantly basinal facies of the Velkerri Formation transitioning up-section to cross-bedded sandstones of the Moroak Sandstone (Fig. 2). The Velkerri Formation is formally divided into three distinct lithostratigraphic members (Munson and Revie, 2018), the Kalala Member, Amungee Member and Wyworrie Member (oldest to youngest, Fig. 2). The Kalala Member has been interpreted as a highly condensed transgressive system tract. The rest of the Velkerri Formation consists of a high stand systems tract, whose top is the base of the overlying Moroak Sandstone (Abbott and Sweet, 2000). The Amungee Member comprises the primary black shale facies, with total organic carbon contents reaching ~10 wt% (Cox et al., 2016; Revie and Normington, 2020)(Figs. 4 & 5) and has been interpreted by astrochronological methods to have been deposited over ca. 10 million years (Mitchell et al., 2020).

Detailed sedimentary petrology of the Amungee Member has shown that the black shale facies was deposited below storm-weather wave-base and is composed of thinly laminated, gray-green to dark gray clays, pale gray silts and rare, fine-grained sands (Warren et al., 1998; Munson, 2016; Munson and Revie, 2018; Sheridan et al., 2018). Organic enrichment within the Amungee Member occurs principally as three prominent horizons informally referred to as the A, B and C organofacies (oldest to youngest)(Figs. 2, 4 & 5). The organic-rich and organic-lean intervals of the Amungee Member show no systematic change in grain size that correlate with TOC enrichment (Warren et al., 1998; Cox et al., 2016). Based on this observation, Warren et al. (1998) noted that these intervals do not reflect changes in the energy of deposition or water depth, but rather changing water column biochemistry. Systematic changes in nitrogen isotopes corresponding to the organofacies suggests that

basin redox and bioavailable nitrogen (the proximal limiting nutrient in most marine systems; Tyrrell, 1999; Bristow et al., 2017), are primary controls on the development of the organofacies (Cox et al., 2019), whereas the enrichment of the Amungee Member as a whole has been related to enhanced phosphorus supply (Cox et al., 2016).

Basin provenance

The Velkerri Formation is sandwiched by two compositionally mature quartz arenites, the underlying Bessie Creek Sandstone and the overlying Moroak Sandstone (Fig. 2). The U–Pb and Hf isotopic composition of detrital zircons within the upper Roper Group show a provenance change from predominately ‘eastern sources’ to ‘southern sources’ (present-day direction) up stratigraphy (Yang et al., 2018; Yang et al., 2019)(Fig. 6). Variation in zircon sourcing broadly reflects an excursion to juvenile neodymium isotope compositions in the Amungee Member shales (Cox et al., 2016). Yang et al. (2018) suggested that this is a reflection of the development of an active margin on the southern side of the North Australian Craton at ca. 1.4 Ga as the Mirning Ocean was subducted, providing nutrients to the McArthur-Yanliao Gulf.

Ecology

The indigenous hydrocarbon biomarker assemblage for the Velkerri Formation has been characterised by Jarrett et al. (2019a), who described a water column dominated by bacteria with large-scale heterotrophic reworking of the organic matter in the water column or bottom sediment. Evidence for microbial reworking includes a large unresolved complex mixture (UCM) and high ratios of monomethyl alkanes relative to *n*-alkanes—features characteristic of indigenous Proterozoic bitumen (Pawlowska et al., 2013). Steranes,

biomarkers for single-celled and multicellular eukaryotes (e.g. Peters et al., 2005; Summons et al., 2006), were below detection limits in all extracts analysed, despite eukaryotic microfossils having been previously identified in the Roper Group (Javaux et al., 2004). This work suggests that eukaryotes, while present, were ecologically restricted and contributed little to the net biomass. This was broadly consistent with preliminary results presented by Flannery and George (2014). The combination of increased dibenzothiophene in the Amungee Member and low concentrations of 2,3,6-trimethyl aryl isoprenoids throughout the Velkerri Formation suggests that the water column at the time of deposition was only transiently euxinic and did not extend into the photic zone. Jarrett et al. (2019a) noted that the biomarker assemblages and water column chemistry of the Velkerri Formation differ markedly from the underlying ca. 1.64 Ga Barney Creek Formation (Brocks et al., 2005; Nettersheim, 2017), demonstrating that microbial environments and water column redox were variable in the Proterozoic and may reflect different depositional environments.

Basin redox

Widely used proxies for basin redox include the redox-sensitive trace metals of cerium, molybdenum and vanadium in black shales (Fig. 7). These metals are useful indicators as they are found in low concentrations (i.e. depleted) under oxidising conditions, but are enriched in sediments under reducing conditions. For example, cerium shows relative depletion compared to its neighbouring rare earth elements (i.e. Ce anomaly) due to its incorporation into ferromanganese nodules/crusts (Elderfield and Greaves, 1981; Nath et al., 1994) upon oxidation of Ce^{3+} to Ce^{4+} . In an analogous fashion, molybdenum exists as the oxidised molybdate ion in seawater (MoO_4^{2-}) but reacts strongly with hydrogen sulfide, such that it is effectively removed from seawater and pore waters under sulfidic (i.e. euxinic)

conditions by incorporation into the sediment. Furthermore, molybdenum also complexes with organic molecules; however, this process still requires hydrogen sulfide of $\sim 10 \mu\text{M}$ (Erickson and Helz, 2000) to quantitatively form particle reactive thiomolybdates (Scott and Lyons, 2012). Similar to molybdenum, vanadium occurs as oxidised V^{5+} as vanadate oxyanions (VO_4^{3-}) under oxic conditions, whereas V^{5+} is reduced by both organic compounds and hydrogen sulfide to V^{4+} under anoxic conditions (Breit and Wanty, 1991), with strong affinities towards organo-metallic complexes (Algeo and Maynard, 2004) and authigenic clays (Peacor et al., 2000).

Due the differing redox potentials of molybdenum and vanadium and coupled redox reactions (i.e. sulfate reduction), V/Mo ratios in shales exhibit distinct changes through the transition from oxic, suboxic, anoxic to euxinic conditions (Piper and Calvert, 2009)(Fig. 7c). Broadly, V/Mo ratios increase through the oxic to suboxic transition while displaying nearly invariant molybdenum concentrations. However, the suboxic to anoxic and then euxinic transition is marked by decreasing V/Mo ratios with increasing molybdenum concentrations.

To date, three prominent basin redox studies have been conducted on the Velkerri Formation, along with data from other Roper Group formations, to suggest a redox structure for the basin. Shen et al. (2003) described deep water anoxia along with oxygenated shallow waters based on iron speciation data, whereas both Cox et al. (2016) and Mukherjee and Large (2016), used trace metals in shales and pyrite respectively, to argue for oxygenated shallow waters, suboxic to anoxic deep waters and intermittent euxinia.

Here we extend these studies by incorporating new data from five wells that form a broad E–W transect across the basin (Tarlee S3, Atree 2, Amungee NW-1H, Tanumbirini 1, Marmbulligan-1; Fig. 1). These data show that redox stratification is persistent across the

basin (Fig. 7). In agreement with previous studies, this redox stratification consists of a shallow oxic layer (Fig. 7 A-B) overlying suboxic to anoxic waters (Fig. 7 C-D). Euxinia is recorded in all five wells and is exclusively associated with high degrees of organic carbon export during deposition of the Amungee Member (Figs. 4, 5, 7 C-D).

These dynamic redox stratified waters are consistent with the prevailing view that Mesoproterozoic basins were characterised by anoxic (ferruginous) to suboxic deep waters, episodic euxinic continental shelves and weakly oxic surface waters (Planavsky et al., 2011; Poulton and Canfield, 2011).

From a source rock perspective, this overall period of widespread suboxic to anoxic relatively deep water implies that deep basins were always conducive to the preservation of organic matter, consequently basin redox fails to explain the onset of organic matter enrichment during deposition of the Amungee Member.

Basin salinity and restriction

Understanding basin dynamics, in particular salinity and restriction is difficult in Precambrian successions, where the full stratigraphic record of the basin is not preserved, as in the case of the Velkerri Formation and broader Roper Group. Donnelly and Crick (1988) inferred deposition of Roper Group sediments within a large lake or silled basin based upon isotopically heavy sulfur values ($\delta^{34}\text{S}$ +3.6‰ to +34.4‰) from disseminated pyrite, inferring a low sulfate environment. A marine origin was proposed based on the wide lateral continuity of Roper Basin sediments (Rawlings, 1999; Rawlings et al., 2004), facies associations and stacking patterns typical for sequence development on a siliciclastic continental shelf, and preserved sedimentary structures typical of open marine deposition (e.g. hummocky and

swaley cross-stratification) (Abbott and Sweet, 2000). However, Munson (2016) noted the common occurrence of syneresis cracks in the Velkerri Formation suggesting that water salinity fluctuated during deposition (Plummer and Gostin, 1981). Considering its intracontinental setting, this sedimentological evidence for changes in salinity and/or connectivity suggests a dynamic interplay between marine/fresh water influx, likely facilitated by tectonically-induced basin restriction/connectivity.

Sulfur in sediments is largely governed by the availability of seawater sulfate, which is coupled to salinity (Berner and Raiswell, 1983; 1984). Carbon-sulfur ratios are sensitive to distinguish between high- and low-sulfate environments and, to a lesser extent, oxic through euxinic settings. These have been validated in both modern (e.g. Berner, 1984; Berner and Raiswell, 1984) and ancient (e.g. Lyons et al., 2000) sedimentary systems. Generally, the supply of sulfate in normal marine settings is not limited, and as long as sufficient organic matter is available for bacterial sulfate reduction, sediments in marine settings are characterised by low C/S ratios. In contrast, freshwater conditions, which favour low dissolved sulfate levels, produce sediments with high C/S ratios (Berner and Raiswell, 1984).

Complications involving C/S ratios exist and include diagenetic, catagenic and metamorphic alteration of both carbon and sulfur, along with the understanding that the reactivity of bulk carbon was likely higher in pre-Silurian sediments due to the absence of lower reactive terrestrial carbon sources (i.e. plant matter, Raiswell and Berner, 1986; Raiswell and Albiatty, 1989; Hieshima and Pratt, 1991), resulting in lower C/S ratios of pre-Silurian sediments.

Carbon and sulfur values from the Velkerri Formation show considerable scatter (Fig. 8), with the majority of data having C/S ratios less than 2.8 (average 2.4 ± 0.5 ; 2σ CI), similar

to modern normal marine waters and an order of magnitude lower than the modern freshwater array (Bernier, 1984; Bernier and Raiswell, 1984).

Due to the greater reactivity of Precambrian organic matter, Lyons et al. (2000) argued that normal open marine Precambrian C/S ratios should be lower than post-Silurian averages (C/S ~ 1.4) and at least equal to (or lower than) Cambrian ratios (C/S ~ 0.5). Excluding a single sample, all Velkerri Formation values have C/S ratios greater than Cambrian ratios, with most values higher than post-Silurian averages. These results preclude a freshwater origin, but, considering the scatter in the dataset, the possibility of enriched sulfur contents due to euxinic samples, and the high salinities recorded in formational (possibly connate) waters from the above lying Moroak Sandstone (Lannigan and Torkington, 1991), salinities somewhere between brackish to normal marine are likely.

Organic carbon isotopes

High total organic carbon (TOC) contents within sediments have been attributed to various factors. These include high primary productivity (Pedersen and Calvert, 1990; Calvert et al., 1996), high nutrient fluxes due to warm and wet climatic conditions (Condie et al., 2001; Meyer and Kump, 2008), basin redox conditions facilitating the preservation of organic matter (Calvert et al., 1996; Hartnett et al., 1998), mineralogical controls on organic carbon export (Mayer, 1994; Hedges and Keil, 1995; Kennedy et al., 2014), and changes in the relative rate of clastic to biogenic sedimentation (Muller and Suess, 1979; Suess, 1980). These processes, which may vary in both space and time, are important in constraining the development of hydrocarbon source rocks.

Measured organic carbon isotope ratios ($\delta^{13}\text{C}_{\text{org}}$) from samples of the organic-rich Amungee Member vary between $\sim -35\text{‰}$ and $\sim -32\text{‰}$. They exhibit a positive correlation with TOC (Fig. 9), such that the most isotopically heavy $\delta^{13}\text{C}$ values are associated with the highest degrees of TOC enrichment. Such a relationship suggests that variations in the siliciclastic flux are not controlling carbon enrichment, as this mechanism would not have an isotopic effect. Also, such organic carbon enrichment is not associated with a maximum flooding surface (Warren et al., 1998; Cox et al., 2019). Considering this, it is likely that the observed $\delta^{13}\text{C}$ variations reflect changes in dissolved inorganic carbon (DIC), or, more specifically, variations in contemporaneous organic carbon burial (f_{org}), which likely reflects the strengthening of primary productivity. Assuming that the observed variations in $\delta^{13}\text{C}_{\text{org}}$ reflect changes in a local DIC reservoir, these could be then translated to changes in the fraction of organic carbon buried (f_{org}) in the McArthur-Yanliao Gulf. The latter can be quantified using a simple carbon isotope mass balance approach for the calculation of f_{org} in the oceans (see Kump et al., 2010). Using modern parameterisation of the marine carbon cycle (i.e. carbon isotope composition of volcanic input of -5‰ to -8‰ , Javoy et al., 1986), the fractionation factor between inorganic and organic carbon of $\sim 23\text{‰}$ to 34‰ (Hayes et al., 1999), and a Monte Carlo simulation approach (see Supplementary Information), data suggest a 3-fold increase in f_{org} to produce the observed change in $\delta^{13}\text{C}_{\text{org}}$.

Source rock characteristics

Using a large data compilation, including the collation in Revie and Normington (2020) and newly generated data in this study ($n=1861$), bootstrapped averages and confidence intervals were calculated on all available pyrolysis data to present an overview of the source rock characteristics of black shales associated with the Velkerri Formation. To assess sample

bias, the data were “jackknifed” (Tukey, 1958) to ensure no individual value(s) significantly biased the data. In all cases, bootstrapped and jackknifed averages are within 7% agreement (or better) of each other (see Supplementary Information). The whole-rock pyrolysis data ($n = 1442$) were filtered to present a more constrained view of source rock characteristics based on the criteria discussed in Hall et al. (2016) and in the supplementary information (Fig. 10). Pyrolysis results may be unreliable for organic-lean samples, or due to the presence of non-indigenous free hydrocarbons—either migrated hydrocarbons or drilling fluid contaminants (Peters, 1986; Dembicki, 2009; Carvajal-Ortiz and Gentzis, 2015). In Amungee NW-1H for example, newly generated T_{\max} values average 320°C (Table 2). These immature values are inconsistent with mud-gas indications in the same intervals that range from 0.29% to 0.67% (Origin Energy Resources Ltd, 2015). Low S₂ values (<0.2 mg HC/g rock) and HI (< 7 mg HC/g rock) are consistent with overmature source rocks and these values were removed during filtering.

Analysis of the black shale facies reveals maximum TOC of ~10 wt%, with an average of 2.65 wt% (± 0.11 ; 2σ CI); TOC varies between wells (Table 2)(Figs. 4 & 5). The classification scheme published by Peters & Casa (1994) categorized rocks with TOC between 1–2 wt% as good source rocks, 2–4 wt% as very good, and > 4 wt% as excellent. Using kernel density estimates to construct the density distribution, Velkerri Formation source rocks should be considered as good to excellent, with most samples considered as good to very good (Fig. 11). The source rock units where TOC >2 wt% typically exceed tens of metres in thickness and can be in excess of 200 metres (e.g. Atree 2, Cox et al., 2016)(Fig. 5). The presence of thick intervals of organic-rich shale is a key aspect of the prospectivity of the Velkerri Formation in the Beetaloo Sub-basin. Productive shale-gas systems generally have TOC >2 wt% and are in excess of 45 m thick (Jarvie, 2012).

Velkerri Formation kerogens contain potential to generate both oil and gas, based on present-day hydrogen indices (HI) of up to 800 mg HC/g TOC (Fig. 11). The average present-day HI is 200 mg HC/g TOC (± 8.4 ; 2σ CI), suggestive of either a gas-prone source rock, or thermally mature sediments (Peters and Cassa, 1994). Results from the thermally immature Marmbulligan well analysed in this study have HI values reaching 551 mg HC/g TOC consistent with an oil- and gas-prone kerogen (Supplementary Information). Trends in hydrogen and oxygen indices are indicative of Type I/II kerogen (Fig. 10 A & D), broadly consistent with previously published results suggesting a bacteria-dominated biomass (Jarrett et al., 2019c; Revie, 2017). Oxygen indices indicate some degradation of organic matter via oxidative processes.

Thermal maturity, as viewed through T_{max} values ranges from immature to overmature, with an average of 438°C (± 1.6 ; 2σ CI) corresponding to relatively low thermal maturity (i.e. oil window)(Fig. 10). Revie (2017) spatially mapped thermal maturity of the Velkerri Formation through the Beetaloo Sub-basin, demonstrating that thermally mature to overmature sediments were situated within the deepest and thickest intersections in the central part of the region where well penetration is limited. Individual well averages diverge from the overall sample population averages. Such divergence is unrelated to sampling density (see Supplementary Information) and likely reflects spatial differences in thermal maturity and original TOC; the former is supported by a statistically significant relationship between HI, S1, Production Index (PI) and depth to intercept (Fig. 12).

Average T_{max} values suggest maturation principally in the oil window, whereas the average present-day HI places maturation in the gas window (Fig. 10). However, T_{max} can be influenced by TOC content, kerogen type and mineral matrix effects (e.g. Espitalie et al., 1980;

Peters, 1986; Dembicki, 2009). An alternative proxy for maturity is the reflectance of organic matter (Dow and O'Connor, 1982). Thermal maturity trends based on both T_{max} and organic reflectance show broad correlations down core in four of the wells analysed in this study (Fig. 13). The discordance between apparently reliable maturity proxies in Velkerri source rocks have been discussed in other studies (Boreham et al., 1988; Faiz et al., 2016; Jarrett et al., 2019c) and suggest that the typical T_{max} thresholds associated with the oil and gas windows may need refining for Precambrian organic matter. We speculate that the overall higher reactivity of bulk Precambrian biomass (Raiswell and Berner, 1986; Raiswell and Albiatty, 1989; Hieshima and Pratt, 1991), and specifically biomass with no terrestrial matter (Tegelaar and Noble, 1994), may be a significant factor for this discordance; this requires further research. To summarize, thick intervals of organic-rich shale occurring in both the oil- and gas-windows are key aspects of the prospectivity of the Velkerri Formation in the Beetaloo Sub-basin. Productive shale-gas systems globally generally have TOC >2 wt%, are in excess of 45 m thick and are within the gas window (Jarvie, 2012). Therefore, the Velkerri Formation meets many of the criteria required for a successful shale-gas play.

Broader earth system implications

Whereas the deposition of organic-rich shales has clear implications for hydrocarbon prospectivity, the geochemistry of the Velkerri Formation has global implications for basin and potentially atmospheric oxygenation, as net oxygen production is fundamentally tied to the burial of organic matter.

The widespread and coeval deposition of black shales in both the McArthur and North Chinese Yanliao basins at ca. 1.38 Ga (Kendall et al., 2006; Zhang et al., 2015; Zhang et al., 2017; Diamond et al., 2018; Mitchell et al., 2020), has been used by a number of studies that

propose an oxygenation event at this time (Cox et al., 2016; Gilleaudeau et al., 2016; Mukherjee and Large, 2016; Zhang et al., 2016; Zhang et al., 2018; Mukherjee et al., 2019). Whether such an oxygenation event was sustained or transient, basin-scale or atmospheric-scale, is a matter of significant debate (Diamond and Lyons, 2018; Planavsky et al., 2018). The concentration of molybdenum in middle Velkerri shales is one of the most convincing lines of evidence for this (possibly transient) oxygenation. Oxidised molybdenum is soluble in oxic waters; however, under euxinic conditions, it is quickly lost from the water column (Reinhard et al., 2013). Consequently, molybdenum concentrations in shales are tied to the oceanic inventory of dissolved molybdenum and more broadly, to both basin and atmospheric redox (Algeo and Lyons, 2006; Scott and Lyons, 2012). Both initial and more recent compilations of molybdenum concentrations reveal that molybdenum rarely exceeds 50 ppm in the Paleoproterozoic or Mesoproterozoic (Scott et al., 2008; Diamond and Lyons, 2018). Velkerri Formation molybdenum concentrations average 59 ppm (± 4 ; 2σ CI), with a maximum of 118 ppm, which suggests that euxinia was not ubiquitous during this period. Consequently, the dissolved molybdenum inventory may have been unusually high at this time in the McArthur-Yanliao Basin, suggesting, at the very least, transiently higher basin and possibly atmospheric oxygen levels.

Implications for hydrocarbon exploration

In many ways, the greater McArthur Basin is not exceptional. Proterozoic basins cover many cratonic areas. For example, the extensive 'Purana' basins of India are similar in terms of age and rock types to the greater McArthur Basin (e.g. Collins et al., 2015). Most of these basins are extremely under-explored.

The example of the Velkerri Formation suggests that high organic horizons correlate with proxies for increased oxia in upper parts of the water column. This introduces an interesting feedback. Increased nutrient supply promotes biomass, which photosynthesises and increases oxygen levels in the upper parts of the ocean. Increased oxia in surface waters means that more oxidised and soluble nutrients such as nitrate (NO_3^-) and phosphate (PO_4^{3-}) remain dissolved in these waters, as do many key nutrients and bio-essential trace metals or micro-nutrients (e.g. Fe, Zn, Cu, Mo, Ni) that are highly redox sensitive. In fact, in an atmosphere with about 1% of the partial pressure of O_2 of today—similar to estimates of the ca. 1500 Ma Earth—marine oxia would occur only in local ‘oxygen oases’ where life blooms (Reinhard et al., 2013). Therefore, source rock quality would be expected to vary considerably along strike within a basin due to variations in nutrient supply.

Conclusions

The Mesoproterozoic Velkerri Formation offers unique insights into Proterozoic paleoenvironments and their hydrocarbon potential. Redox stratification was persistent across the basin and consisted of a shallow oxic layer with deeper water suboxic to anoxic conditions that were episodically euxinic. The biomass was dominated by bacteria and multiple lines of evidence suggest that organic enrichment is related to high degrees of primary productivity associated with conducive biogeochemical conditions. Although deposited in an intra-continental setting, the sedimentology, paleosalinity and palaeoredox conditions of the basin support global reconstructions that have the Velkerri Formation lying within a large embayment of the supercontinent Nuna, that we call the McArthur-Yanliao Gulf. These reconstructions, combined with available age constraints, tie the deposition of the Velkerri Formation with a period of more widespread deposition of black shales within

this gulf that may reflect high biological productivity that endogenously oxygenated surface waters in a low atmospheric oxygen world. This may reflect local basin conditions in a Baltic Sea-like environment (e.g. Markus Meier et al., 2021) or possibly may reflect a transient global increase in atmospheric oxygen (Mukherjee and Large, 2016).

References

- Abbott, S. T., and I. P. Sweet, 2000, Tectonic control on third-order sequences in a siliciclastic ramp-style basin: an example from the Roper Superbasin (Mesoproterozoic), northern Australia: *Australian Journal of Earth Sciences*, v. 47, p. 637-657.
- Algeo, T. J., and T. W. Lyons, 2006, Mo-total organic carbon covariation in modern anoxic marine environments: Implications for analysis of paleoredox and paleohydrographic conditions: *Paleoceanography*, v. 21.
- Algeo, T. J., and J. B. Maynard, 2004, Trace-element behavior and redox facies in core shales of Upper Pennsylvanian Kansas-type cyclothems: *Chemical Geology*, v. 206, p. 289-318.
- Baruch, E. T., C. M. Altmann, D. I. Close, F. M. Mohinudeen, B. A. Richards, and A. J. Côte, 2018, The Kyalla Formation prospectivity from a mineralogical and sedimentological perspective: *AGES 2018*, p. 40-48.
- Berner, R. A., 1984, Sedimentary Pyrite Formation - an Update: *Geochimica Et Cosmochimica Acta*, v. 48, p. 605-615.
- Berner, R. A., and R. Raiswell, 1983, Burial of Organic-Carbon and Pyrite Sulfur in Sediments over Phanerozoic Time - a New Theory: *Geochimica Et Cosmochimica Acta*, v. 47, p. 855-862.
- Berner, R. A., and R. Raiswell, 1984, C/S Method for Distinguishing Fresh-Water from Marine Sedimentary-Rocks: *Geology*, v. 12, p. 365-368.
- Bodorkos, S., J. L. Crowley, J. C. Clauoué-Long, J. R. Anderson, and C. W. J. Magee, 2020, Precise U–Pb baddeleyite dating of the Derim Derim Dolerite, McArthur Basin, Northern Territory: old and new SHRIMP and ID-TIMS constraints: *Australian Journal of Earth Sciences*, v. 68, p. 36-50.
- Boreham, C. J., I. H. Crick, and T. G. Powell, 1988, Alternative Calibration of the Methylphenanthrene Index against Vitrinite Reflectance - Application to Maturity Measurements on Oils and Sediments: *Organic Geochemistry*, v. 12, p. 289-294.
- Breit, G. N., and R. B. Wanty, 1991, Vanadium Accumulation in Carbonaceous Rocks - a Review of Geochemical Controls during Deposition and Diagenesis: *Chemical Geology*, v. 91, p. 83-97.

- Bristow, L. A., W. Mohr, S. Ahmerkamp, and M. M. M. Kuypers, 2017, Nutrients that limit growth in the ocean: *Current Biology*, v. 27, p. R474-R478.
- Brocks, J. J., G. D. Love, R. E. Summons, A. H. Knoll, G. A. Logan, and S. A. Bowden, 2005, Biomarker evidence for green and purple sulphur bacteria in a stratified Palaeoproterozoic sea: *Nature*, v. 437, p. 866-870.
- Calvert, S. E., R. M. Bustin, and E. D. Ingall, 1996, Influence of water column anoxia and sediment supply on the burial and preservation of organic carbon in marine shales: *Geochimica Et Cosmochimica Acta*, v. 60, p. 1577-1593.
- Carvajal-Ortiz, H., and T. Gentzis, 2015, Critical considerations when assessing hydrocarbon plays using Rock-Eval pyrolysis and organic petrology data: Data quality revisited: *International Journal of Coal Geology*, v. 152, p. 113-122.
- Cawood, P. A., W. Wang, T. Zhao, Y. Xu, J. A. Mulder, S. A. Pisarevsky, L. Zhang, C. Gan, H. Hee, H. Liu, L. Qi, Y. Wang, J. Yao, G. Zhao, M.-F. Zhou, and J.-W. Zi, 2020, Deconstructing South China and consequences for reconstructing Nuna and Rodinia: *Earth Science Reviews*, v. 204, p. 103169.
- Close, D. F., 2014, The McArthur Basin: NTGS' approach to a frontier petroleum basin with known base metal prospectivity: in 'Annual Geoscience Exploration Seminar (AGES) 2014. Record of abstracts', Northern Territory Geological Survey, Record 2014-001. <https://geoscience.nt.gov.au/gemis/ntgsjspui/handle/1/81540>.
- Close, D. I., A. J. Côte, E. T. Baruch, C. M. Altmann, F. M. Mohinudeen, B. Richards, and R. Ilett, 2017, Proterozoic shale gas plays in the Beetaloo Basin and the Amungee NW-1H discovery, in Annual Geoscience Exploration Seminar (AGES) Proceedings, Alice Springs, Northern Territory, 28–29 March 2017. Northern Territory Geological Survey, Darwin. <https://geoscience.nt.gov.au/gemis/ntgsjspui/handle/1/85149>.
- Collins, A. S., J. Farkas, S. Glorie, M. L. Blades, G. M. Cox, J. D. Foden, A. Hall, J. L. Payne, B. Yang, A. Nixon, E. Cassidy, D. Subarkah, A. Shannon, D. Higgie, G. Toledo, A. Dosseto, U. Kirscher, C. Edgoose, D. Close, T. J. Munson, S. Menpes, S. Spagnuolo, D. Close, E. Baruch-Jurado, J. Warburton, and G. Hokin, 2019, Life and times of the Proterozoic McArthur-Yanliao Gulf: Update on the ARC-Industry-NTGS Linkage Project: in Annual Geoscience Exploration Seminar (AGES) Proceedings, Alice Springs, Northern Territory, 19–20 March 2019. Northern Territory Geological Survey, Darwin. <https://geoscience.nt.gov.au/gemis/ntgsjspui/handle/1/88334>.
- Collins, A. S., S. Patranabis-Deb, E. Alexander, C. Bertram, G. Falster, R. Gore, J. Mackintosh, P. C. Dhang, D. Saha, J. Payne, J., F. Jourdan, G. Backé, G. P. Halverson, B. P. Wade, 2015. Detrital Mineral Age, Radiogenic Isotopic Stratigraphy and Tectonic Significance of the Cuddapah Basin, India: *Gondwana Research*, v. 28, p. 1294-1309.
- Condie, K. C., D. J. Des Marais, and A. Dallas, 2001, Precambrian superplumes and supercontinents; a record in black shales, carbon isotopes, and paleoclimates: *Precambrian Research*, v. 106, p. 239-260.

- Cox, G. M., A. Jarrett, D. Edwards, P. W. Crockford, G. P. Halverson, A. S. Collins, A. Poirier, and Z. X. Li, 2016, Basin redox and primary productivity within the Mesoproterozoic Roper Seaway: *Chemical Geology*, v. 440, p. 101-114.
- Cox, G. M., P. Sansjofre, M. L. Blades, J. Farkas, and A. S. Collins, 2019, Dynamic interaction between basin redox and the biogeochemical nitrogen cycle in an unconventional Proterozoic petroleum system: *Scientific Reports*, v. 9.
- Crick, I. H., C. J. Boreham, A. C. Cook, and T. G. Powell, 1988, Petroleum Geology and Geochemistry Of Middle Proterozoic McArthur Basin, Northern Australia .2. Assessment Of Source Rock Potential: *AAPG Bulletin-American Association Of Petroleum Geologists*, v. 72, p. 1495-1514.
- Dembicki, H., 2009, Three common source rock evaluation errors made by geologists during prospect or play appraisals: *Aapg Bulletin*, v. 93, p. 341-356.
- Diamond, C. W., and T. W. Lyons, 2018, Mid-Proterozoic redox evolution and the possibility of transient oxygenation events: *Emerging Topics in Life Sciences*, v. 2, p. 235-245.
- Diamond, C. W., N. J. Planavsky, C. Wang, and T. W. Lyons, 2018, What the ~1.4 Ga Xiamaling Formation can and cannot tell us about the mid-Proterozoic ocean: *Geobiology*, v. 16, p. 219-236.
- Donnelly, T. H., and I. H. Crick, 1988, Depositional Environment of the Middle Proterozoic Velkerri Formation in Northern Australia - Geochemical Evidence: *Precambrian Research*, v. 42, p. 165-172.
- Dow, W. G., and D. I. O'Connor, 1982, Kerogen maturity and type by reflected light microscopy applied to petroleum exploration, *in* F. L. Staplin, W. G. Dow, C. W. D. Milner, D. I. O'Connor, S. A. J. Pocock, P. van Gijssel, D. H. Welte, and M. A. Yukler, eds., *How to Assess Maturation and Paleotemperatures*, v. S.E.P.M. Short Course 7: Tulsa, Society for Sedimentary Geology, p. 133-157.
- Elderfield, H., and M. J. Greaves, 1981, Negative Cerium Anomalies in the Rare-Earth Element Patterns of Oceanic Ferromanganese Nodules: *Earth and Planetary Science Letters*, v. 55, p. 163-170.
- Erickson, B. E., and G. R. Helz, 2000, Molybdenum(VI) speciation in sulfidic waters: Stability and lability of thiomolybdates: *Geochimica et Cosmochimica Acta*, v. 64, p. 1149-1158.
- Espitalie, J., M. Madec, and B. Tissot, 1980, Role of Mineral Matrix in Kerogen Pyrolysis - Influence on Petroleum Generation and Migration: *AAPG Bulletin*, v. 64, p. 59-66.
- Faiz, M., C. Altmann, D. Michael, E. Baruch-Jurado, D. Close, A. Cote, R. Richards, and R. Paddy, 2016, Precambrian Organic matter and Thermal Maturity of the Beetaloo Basin, Northern Territory, Australia., Australian Earth Sciences Convention, Adelaide
- Fanning C. M., 2012, SHRIMP U-Pb zircon age determinations on detrital zircons from drill core sample ALT-051. ANU Research School of Earth Sciences, PRISE Report 12-260. Esso Australia. Northern Territory Geological Survey, Core Sampling Report CSR0211. <https://geoscience.nt.gov.au/gemis/ntgsjspui/handle/1/84919>

- Flannery, E. N., and S. C. George, 2014, Assessing the syngeneity and indigeneity of hydrocarbons in the similar to 1.4 Ga Velkerri Formation, McArthur Basin, using slice experiments: *Organic Geochemistry*, v. 77, p. 115-125.
- Frogtech Geoscience, 2018, SEEBASE® study and GIS for greater McArthur Basin. Northern Territory Geological Survey, Digital Information Package DIP 017. <https://geoscience.nt.gov.au/gemis/ntgsjspui/handle/1/87064>
- Gilleaudeau, G. J., R. Frei, A. J. Kaufman, L. C. Kah, K. Azmy, J. K. Bartley, P. Chernyavskiy, and A. H. Knoll, 2016, Oxygenation of the mid-Proterozoic atmosphere: clues from chromium isotopes in carbonates: *Geochemical Perspectives Letters*, v. 2, p. 178-+.
- Hall, L. S., C. J. Boreham, D. S. Edwards, T. J. Palu, T. Buckler, A. J. Hill, and A. Troup, 2016, Cooper Basin Source Rock Geochemistry: Regional Hydrocarbon Prospectivity of the Cooper Basin, Part 2., Canberra.
- Hartnett, H. E., R. G. Keil, J. I. Hedges, and A. H. Devol, 1998, Influence of oxygen exposure time on organic carbon preservation in continental margin sediments: *Nature*, v. 391, p. 572-574.
- Hayes, J. M., H. Strauss, and A. J. Kaufman, 1999, The abundance of C-13 in marine organic matter and isotopic fractionation in the global biogeochemical cycle of carbon during the past 800 Ma: *Chemical Geology*, v. 161, p. 103-125.
- Hedges, J. I., and R. G. Keil, 1995, Sedimentary Organic-Matter Preservation - an Assessment and Speculative Synthesis: *Marine Chemistry*, v. 49, p. 81-115.
- Hieshima, G. B., and L. M. Pratt, 1991, Sulfur Carbon Ratios and Extractable Organic-Matter of the Middle Proterozoic Nonesuch Formation, North-American Midcontinent Rift: *Precambrian Research*, v. 54, p. 65-79.
- Jackson, M. J., T. G. Powell, R. E. Summons, and I. P. Sweet, 1986, Hydrocarbon Shows and Petroleum Source Rocks in Sediments as Old as 1.7×10^9 Years: *Nature*, v. 322, p. 727-729.
- Jarrett, A. J. M., G. M. Cox, J. J. Brocks, E. Grosjean, C. J. Boreham, and D. S. Edwards, 2019a, Microbial assemblage and palaeoenvironmental reconstruction of the 1.38 Ga Velkerri Formation, McArthur Basin, northern Australia: *Geobiology*, v. 17, p. 360-380.
- Jarrett, A. J. M., Z. Hong, N. Jinadasa, J. Anderson, J. Chen, and P. Henson, 2019b, Exploring for the Future- Source rock geochemistry of Northern Australia. Data Release 2: Total organic carbon (TOC) and Rock-Eval pyrolysis of samples from the McArthur, South Nicholson Basin and Isa Superbasin, Northern Territory, Canberra, p. 1-32.
- Jarrett, A. J. M., S. MacFarlane, T. Palu, C. Boreham, L. Hall, D. Edwards, G. Cox, J. Brocks, T. Munson, L. K. Carr, and P. Henson, 2019c, Source rock geochemistry and petroleum systems of the greater McArthur Basin and links to other northern Australian Proterozoic basins: in Annual Geoscience Exploration Seminar (AGES) Proceedings, Alice Springs, Northern Territory, 19–20 March 2019. Northern

Territory Geological Survey, Darwin.
<https://geoscience.nt.gov.au/gemis/ntgsjspui/handle/1/88334>.

- Jarvie, D., 2018, Correlation of Tmax and measured vitrinite reflectance., TCU Energy Inst.
- Jarvie, D. M., 2012, Shale resource systems for oil and gas: Part 1: Shale-gas resource systems, *in* J. A. Breyer, ed., Shale reservoirs--Giant resources for the 21st century, v. AAPG Memoir 97, AAPG, p. 69-87.
- Javaux, E. J., A. H. Knoll, and M. R. Walter, 2004, TEM evidence for eukaryotic diversity in mid-Proterozoic oceans: *Geobiology*, v. 2, p. 121-132.
- Javoy, M., F. Pineau, and H. Delorme, 1986, Carbon and Nitrogen Isotopes in the Mantle: *Chemical Geology*, v. 57, p. 41-62.
- Kendall, B., R. A. Creaser, G. W. Gordon, and A. D. Anbar, 2009, Re-Os and Mo isotope systematics of black shales from the Middle Proterozoic Velkerri and Wollogorang Formations, McArthur Basin, northern Australia: *Geochimica et Cosmochimica Acta*, v. 73, p. 2534-2558.
- Kendall, B., R. A. Creaser, and D. Selby, 2006, Re-Os geochronology of postglacial black shales in Australia: Constraints on the timing of "Sturtian" glaciation: *Geology*, v. 34, p. 729-732.
- Kennedy, M. J., S. C. Lohr, S. A. Fraser, and E. T. Baruch, 2014, Direct evidence for organic carbon preservation as clay-organic nanocomposites in a Devonian black shale; from deposition to diagenesis: *Earth and Planetary Science Letters*, v. 388, p. 59-70.
- Kirscher, U., R. Mitchell, Y. Liu, Z. X. Li, G. M. Cox, A. Nordsvan, C. Wang, and S. Pisarevsky, 2018, Long lived supercontinent Nuna - updated paleomagnetic constraints from Australia, AGU Fall Meeting.
- Kump, L. R., J. F. Kasting, and R. G. Crane, 2010, *The Earth System*: New Jersey, Prentice Hall, 419 p.
- Lannigan, K., and J. Torkington, 1991, Well Completion Report EP 18 - Jamison 1 Beetaloo Sub-Basin of the McArthur Basin. Pacific Oil & Gas Pty Ltd. Northern Territory Geological Survey, Open File Petroleum Report PR1991-0020.
<https://geoscience.nt.gov.au/gemis/ntgsjspui/handle/1/79447>.
- Lyons, T. W., J. J. Luepke, M. E. Schreiber, and G. A. Zieg, 2000, Sulfur geochemical constraints on Mesoproterozoic restricted marine deposition: lower Belt Supergroup, northwestern United States: *Geochimica Et Cosmochimica Acta*, v. 64, p. 427-437.
- Markus Meier, H. E., C. Dieterich, and M. Gröger, 2021, Natural variability is a large source of uncertainty in future projections of hypoxia in the Baltic Sea: *Communications Earth & Environment*, v. 2, p. 50.
- Mayer, L. M., 1994, Surface-Area Control of Organic-Carbon Accumulation in Continental-Shelf Sediments: *Geochimica et Cosmochimica Acta*, v. 58, p. 1271-1284.

- Meyer, K. M., and L. R. Kump, 2008, Oceanic euxinia in Earth history: Causes and consequences: *Annual Review of Earth and Planetary Sciences*, v. 36, p. 251-288.
- Mitchell, R. N., U. Kirscher, M. Kunzmann, Y. Liu, and G. M. Cox, 2020, Gulf of Nuna: Astrochronologic correlation of a Mesoproterozoic oceanic euxinic event: *Geology*, v. 48, p. <https://doi.org/10.1130/G47587.1>.
- Mukherjee, I., and R. R. Large, 2016, Pyrite trace element chemistry of the Velkerri Formation, Roper Group, McArthur Basin: Evidence for atmospheric oxygenation during the Boring Billion: *Precambrian Research*, v. 281, p. 13-26.
- Mukherjee, I., R. R. Large, S. Bull, D. G. Gregory, A. S. Stepanov, J. Avila, T. R. Ireland, and R. Corkrey, 2019, Pyrite trace-element and sulfur isotope geochemistry of paleo-mesoproterozoic McArthur Basin: Proxy for oxidative weathering: *American Mineralogist*, v. 104, p. 1256-1272.
- Muller, P. J., and E. Suess, 1979, Productivity, Sedimentation-Rate, and Sedimentary Organic-Matter in the Oceans .1. Organic-Carbon Preservation: *Deep-Sea Research Part a-Oceanographic Research Papers*, v. 26, p. 1347-1362.
- Munson, T. J., 2016, Sedimentary characterisation of the Wilton package, greater McArthur Basin. Northern Territory: Northern Territory Geological Survey, Record, v. 2016-003. <https://geoscience.nt.gov.au/gemis/ntgsjspui/handle/1/83806>
- Munson, T. J., and D. Revie, 2018, Stratigraphic subdivision of the Velkerri Formation, Roper Group, McArthur Basin, Northern Territory.: Northern Territory Geological Survey Record v. 2018-006. <https://geoscience.nt.gov.au/gemis/ntgsjspui/handle/1/87322>
- Munson T. J., Thompson J. M., Zhukova I., Meffre S., Beyer E. E., Woodhead J. D. and Whelan J. A , 2018, Summary of results. NTGS laser ablation ICP–MS U–Pb and Lu–Hf geochronology project: Roper Group (McArthur Basin), overlying ungrouped units (Beetaloo Sub-basin), Renner Group (Tomkinson Province), and Tijnuna Group (Birrindudu Basin). Northern Territory Geological Survey, Record 2018-007. <https://geoscience.nt.gov.au/gemis/ntgsjspui/handle/1/87656>
- Nance, W. B., and S. R. Taylor, 1976, Rare earth element patterns and crustal evolution - II. Archean sedimentary rocks from Kalgoorlie, Australia.: *Geochem and Cosmochem Acta.*, v. 40, p. 1539-1551.
- Nath, B. N., I. Roelandts, M. Sudhakar, W. L. Pluger, and V. Balaram, 1994, Cerium Anomaly Variations in Ferromanganese Nodules and Crusts from the Indian-Ocean: *Marine Geology*, v. 120, p. 385-400.
- Nettersheim, B. J., 2017, Reconstructing Earth's alien ancient ecology- A multiproxy study of the 1.64 billion-year old Barney Creek Formation, northern Australia. Unpublished PhD Thesis, Australian National University, Canberra.
- Origin Energy Resources Ltd, 2015, Amungee NW-1, Well Completion Report, EP 98, Beetaloo Basin, Northern Territory. Northern Territory Geological Survey, Open File Petroleum Report PR2016-W012. <https://geoscience.nt.gov.au/gemis/ntgsjspui/handle/1/86845>

- Page, R. W., M. J. Jackson, and A. A. Krassay, 2000, Constraining sequence stratigraphy in north Australian basins: SHRIMP U-Pb zircon geochronology between Mt Isa and McArthur River: *Australian Journal of Earth Sciences*, v. 47, p. 431-459.
- Pawlowska, M. M., N. J. Butterfield, and J. J. Brocks, 2013, Lipid taphonomy in the Proterozoic and the effect of microbial mats on biomarker preservation: *Geology*, v. 41, p. 103-106.
- Peacor, D. R., R. M. Coveney, and G. M. Zhao, 2000, Authigenic illite and organic matter: The principal hosts of vanadium in the Mecca Quarry Shale at Velpen, Indiana: *Clays and Clay Minerals*, v. 48, p. 311-316.
- Pedersen, T. F., and S. E. Calvert, 1990, Anoxia Vs Productivity - What Controls the Formation of Organic-Carbon-Rich Sediments and Sedimentary-Rocks: *Aapg Bulletin-American Association of Petroleum Geologists*, v. 74, p. 454-466.
- Peters, K. E., 1986, Guidelines for Evaluating Petroleum Source Rock Using Programmed Pyrolysis: *Aapg Bulletin-American Association of Petroleum Geologists*, v. 70, p. 318-329.
- Peters, K. E., and M. R. Cassa, 1994, Applied Source-Rock Geochemistry, *in* L. B. Magoon, and W. G. Dow, eds., *The Petroleum System: From Source to Trap*: Tulsa, American Association of Petroleum Geologists, p. 93-120.
- Peters, K. E., C. C. Walters, and M. J. Moldowan, 2005, *The Biomarker Guide. Volume 1: Biomarkers and Isotopes in the Environment and Human History. Volume 2: Biomarkers and Isotopes in Petroleum Exploration and Earth History. 2nd edition*: Cambridge, Cambridge University Press, 1132 p.
- Piper, D. Z., and S. E. Calvert, 2009, A marine biogeochemical perspective on black shale deposition: *Earth-Science Reviews*, v. 95, p. 63-96.
- Planavsky, N. J., D. B. Cole, T. T. Isson, C. T. Reinhard, P. W. Crockford, N. D. Sheldon, and T. W. Lyons, 2018, A case for low atmospheric oxygen levels during Earth's middle history: *Emerging Topics in Life Sciences*, v. 2, p. 149-159.
- Planavsky, N. J., P. McGoldrick, C. T. Scott, C. Li, C. T. Reinhard, A. E. Kelly, X. L. Chu, A. Bekker, G. D. Love, and T. W. Lyons, 2011, Widespread iron-rich conditions in the mid-Proterozoic ocean: *Nature*, v. 477, p. 448-U95.
- Plumb, K. A., and H. G. Roberts, 1992, *The geology of Arnhem Land, Northern Territory*: Bureau of Mineral Resources, Australia v. Record 1992/55.
- Plumb, K. A., and P. Wellman, 1987, McArthur Basin, Northern Territory: mapping of deep troughs using gravity and magnetic anomalies: *Journal of Australian Geology and Geophysics*, v. 10, p. 243-251.
- Plummer, P. S., and V. A. Gostin, 1981, Shrinkage Cracks - Desiccation or Synaeresis: *Journal of Sedimentary Petrology*, v. 51, p. 1147-1156.
- Poulton, S. W., and D. E. Canfield, 2011, Ferruginous Conditions: A Dominant Feature of the Ocean through Earth's History: *Elements*, v. 7, p. 107-112.

- Raiswell, R., and H. J. Albiatty, 1989, Depositional and Diagenetic C-S-Fe Signatures in Early Paleozoic Normal Marine Shales: *Geochimica et Cosmochimica Acta*, v. 53, p. 1147-1152.
- Raiswell, R., and R. A. Berner, 1986, Pyrite and Organic-Matter in Phanerozoic Normal Marine Shales: *Geochimica Et Cosmochimica Acta*, v. 50, p. 1967-1976.
- Rawlings, D. J., 1999, Stratigraphic resolution of a multiphase intracratonic basin system: the McArthur Basin, northern Australia: *Australian Journal of Earth Sciences*, v. 46, p. 703-723.
- Rawlings, D. J., R. J. Korsch, B. R. Goleby, G. M. Gibson, D. W. Johnstone, M. Barlow, and 2004, 78 p., 2004, The 2002 Southern McArthur Basin Seismic Reflection Survey: *Geoscience Australia, Record 2004/17*.
- Raymond, O. L., J. M. Totterdell, A. J. Stewart, and M. A. Woods, 2018, Australian Geological Provinces 2018.01 edition, *in* G. Australia, ed., Canberra.
- Reinhard, C. T., N. J. Planavsky, L. J. Robbins, C. A. Partin, B. C. Gill, S. V. Lalonde, A. Bekker, K. O. Konhauser, and T. W. Lyons, 2013, Proterozoic ocean redox and biogeochemical stasis: *Proceedings of the National Academy of Sciences of the United States of America*, v. 110, p. 5357-5362.
- Revie, D., 2017, Unconventional petroleum resources of the Roper Group, McArthur Basin. Northern Territory Geological Survey, Record 2017-002.
<https://geoscience.nt.gov.au/gemis/ntgsjspui/handle/1/85134>, p. 64.
- Revie, D., and V. J. Normington, 2020, Shale resource data from the greater McArthur Basin: Northern Territory Geological Survey: Digital Information Package, v. DIP-014. .
<https://geoscience.nt.gov.au/gemis/ntgsjspui/handle/1/82595>
- Schneck, C. J., T. J. Mercier, C. A. Woodall, T. M. Finn, K. R. Marra, M. E. Brownfield, H. M. Leathers-Miller, and R. D. I. Drake, 2019, Assessment of continuous oil and gas resources in the Beetaloo Basin, Australia: *U.S. Geological Survey Fact Sheet 2019-3013*.
- Scott, C., and T. W. Lyons, 2012, Contrasting molybdenum cycling and isotopic properties in euxinic versus non-euxinic sediments and sedimentary rocks: Refining the paleoproxies: *Chemical Geology*, v. 324, p. 19-27.
- Scott, C., T. W. Lyons, A. Bekker, Y. Shen, S. W. Poulton, X. Chu, and A. D. Anbar, 2008, Tracing the stepwise oxygenation of the Proterozoic ocean: *Nature*, v. 452, p. 456-U5.
- Shen, Y., A. H. Knoll, and M. R. Walter, 2003, Evidence for low sulphate and anoxia in a mid-Proterozoic marine basin: *Nature*, v. 423, p. 632-635.
- Sheridan, M., R. D. Johns, H. D. Johnson, and S. Menpes, 2018, The stratigraphic architecture, distribution and hydrocarbon potential of the organic-rich Kyalla and Velkerri shales of the Upper Roper Group (McArthur Basin): *The APPEA Journal*, v. 58, p. 858-864.

- Spinks, S. C., S. Schmid, and A. Pages, 2016, Delayed euxinia in Paleoproterozoic intracontinental seas: Vital havens for the evolution of eukaryotes?: *Precambrian Research*, v. 287, p. 108-114.
- Suess, E., 1980, Particulate Organic-Carbon Flux in the Oceans - Surface Productivity and Oxygen Utilization: *Nature*, v. 288, p. 260-263.
- Summons, R. E., A. S. Bradley, L. L. Jahnke, and J. R. Waldbauer, 2006, Steroids, triterpenoids and molecular oxygen: *Philosophical Transactions of the Royal Society B-Biological Sciences*, v. 361, p. 951-968.
- Tegelaar, E. W., and R. A. Noble, 1994, Kinetics of Hydrocarbon Generation as a Function of the Molecular-Structure of Kerogen as Revealed by Pyrolysis-Gas Chromatography: *Organic Geochemistry*, v. 22, p. 543-574.
- Tukey, J. W., 1958, Bias and Confidence in Not-Quite Large Samples: *Annals of Mathematical Statistics*, v. 29, p. 614-614.
- Tyrrell, T., 1999, The relative influences of nitrogen and phosphorus on oceanic primary production: *Nature*, v. 400, p. 525-531.
- Warren, J. K., S. C. George, P. J. Hamilton, and P. Tingate, 1998, Proterozoic source rocks: Sedimentology and organic characteristics of the Velkerri Formation, Northern Territory, Australia: *AAPG Bulletin*, v. 82, p. 442-463.
- Williams, B., 2019, Definition of the Beetaloo Sub-basin, Northern Territory Geological Survey, Record 2019-015.
<https://geoscience.nt.gov.au/gemis/ntgsjspui/handle/1/89822>
- Yang, B., A. S. Collins, M. L. Blades, N. Capogreco, J. L. Payne, T. J. Munson, G. M. Cox, and S. Glorie, 2019, Middle-late Mesoproterozoic tectonic geography of the North Australia Craton: U-Pb and Hf isotopes of detrital zircon grains in the Beetaloo Sub-basin, Northern Territory, Australia: *Journal of the Geological Society*, v. 176, p. 771-784.
- Yang, B., A. S. Collins, G. M. Cox, A. J. M. Jarrett, S. Denyszyn, M. L. Blades, Y. Farkaš, and S. Glorie, 2020, Using Mesoproterozoic Sedimentary Geochemistry to Reconstruct Basin Tectonic Geography and Link Organic Carbon Productivity to Nutrient Flux from a Northern Australian Large Igneous Province: *Basin Research*, v. 32.
- Yang, B., T. M. Smith, A. S. Collins, T. J. Munson, B. Schoemaker, D. Nicholls, G. Cox, J. Farkas, and S. Glorie, 2018, Spatial and temporal variation in detrital zircon age provenance of the hydrocarbon-bearing upper Roper Group, Beetaloo Sub-basin, Northern Territory, Australia: *Precambrian Research*, v. 304, p. 140-155.
- Zhang, K., X. K. Zhu, R. A. Wood, Y. Shi, Z. F. Gao, and S. W. Poulton, 2018, Oxygenation of the Mesoproterozoic ocean and the evolution of complex eukaryotes: *Nature Geoscience*, v. 11, p. 345-350.
- Zhang, S. C., X. M. Wang, E. U. Hammarlund, H. J. Wang, M. M. Costa, C. J. Bjerrum, J. N. Connelly, B. M. Zhang, L. Z. Bian, and D. E. Canfield, 2015, Orbital forcing of

climate 1.4 billion years ago: Proceedings of the National Academy of Sciences of the United States of America, v. 112, p. E1406-E1413.

Zhang, S. C., X. M. Wang, H. J. Wang, C. J. Bjerrum, E. U. Hammarlund, M. M. Costa, J. N. Connelly, B. M. Zhang, J. Su, and D. E. Canfield, 2016, Sufficient oxygen for animal respiration 1,400 million years ago: Proceedings of the National Academy of Sciences of the United States of America, v. 113, p. 1731-1736.

Zhang, S. H., Y. Zhao, X. H. Li, R. E. Ernst, and Z. Y. Yang, 2017, The 1.33-1.30 Ga Yanliao large igneous province in the North China Craton: Implications for reconstruction of the Nuna (Columbia) supercontinent, and specifically with the North Australian Craton: Earth and Planetary Science Letters, v. 465, p. 112-125.

Authors

Grant Cox worked as a post-doctoral research fellow at The University of Adelaide after undertaking a PhD at McGill University, Canada. He worked at Adelaide as a geochemist on unravelling the nature of the Proterozoic earth.

Alan S. Collins is a professor at The University of Adelaide. He leads the Tectonics and Earth Systems Group (TES) and his research is focused on understanding the interplay between plate tectonics, tectonic geography and earth surface systems in deep time.

Amber J.M. Jarrett is a petroleum geochemist at the Northern Territory Geological Survey specialising in Proterozoic aged basins. Amber graduated with a BSc (Hons), majoring in both Geology and Biology, in 2008 and a PhD in 2014 from the Australian National University (ANU) and worked as a petroleum geochemist at Geoscience Australia from 2014 to 2020.

Morgan L. Blades graduated with Honours from the University of Adelaide in 2013, then undertook a PhD focussed on the tectonic evolution of the northern East African Orogen. Since 2017 she has been employed as a research fellow with the greater McArthur Basin consortia.

April V. Shannon was an Honours student at The University of Adelaide. For her thesis, she worked on the organic geochemistry of the greater McArthur Basin.

Bo Yang obtained his PhD in 2019 from the University of Adelaide, Australia. After the graduation, he worked as a post-doctoral researcher at The University of Adelaide. His current research interests are in the linking of sedimentary geochronology and chemistry with the formation and evolution of basin geography in order to constrain regional tectonics.

Juraj Farkas' research interest is focused on the application of metal isotopes and novel analytical techniques to low-temperature geochemistry, including earth system evolution studies, and isotope tracing of metals in near-surface environments. He completed his PhD at University of Ottawa, Canada, followed by postdoctoral training at Harvard, USA, and recently established Metal Isotope Group at University of

Adelaide, Australia.

Phillip A. Hall (Tony) is a mass spectrometry specialist with over 15 yrs experience in commercial GLP, UKAS & ISO accredited laboratories prior to undertaking a PhD at University of Adelaide. Primarily an organic geochemist with interests in petroleum exploration these have expanded into biofuels and biochars, soils and their related bacterial communities, palaeoclimatology, plant research and animal welfare.

Brendan O'Hara graduated in 2000 from Queen's University, Northern Ireland. From 2005 to 2014 he worked in Alberta, Canada, across the foreland basin from backbulge to foredeep basin oil and gas plays. In 2014, he moved to Australia and worked in the Cooper Basin and before taking on the McArthur Basin challenges.

David Close is currently the General Manager for Near Field Exploration at Santos in Brisbane, Australia. He holds a Ph.D. from the University of Oxford and a B.Sc. from the University of Tasmania. David has worked across a number of basins and play types in Mexico, U.S.A, Canada and Australia for Schlumberger, Apache Canada, Origin and Santos.

Elizabeth T. Baruch is an Exploration Geologist for Origin Energy in Brisbane, Australia. She received her B.Sc. degree from Simon Bolivar University (Venezuela), M.Sc. from the University of Oklahoma and is currently a Ph.D. candidate at the University of Adelaide. She has worked in unconventional exploration roles with expertise in shale gas, shale diagenesis and sedimentology.

Acknowledgements

All authors would like to thank the Northern Territory Geological Survey (NTGS), Santos Limited, Origin Energy and Imperial Oil and Gas for access to core and data in addition to Tim Munson and Marcus Kunzmann for valuable comments on an earlier version of this manuscript. ASC, GMC and MLB are supported by an Australian Research Council Linkage Grant LP160101353.

Figures and Tables

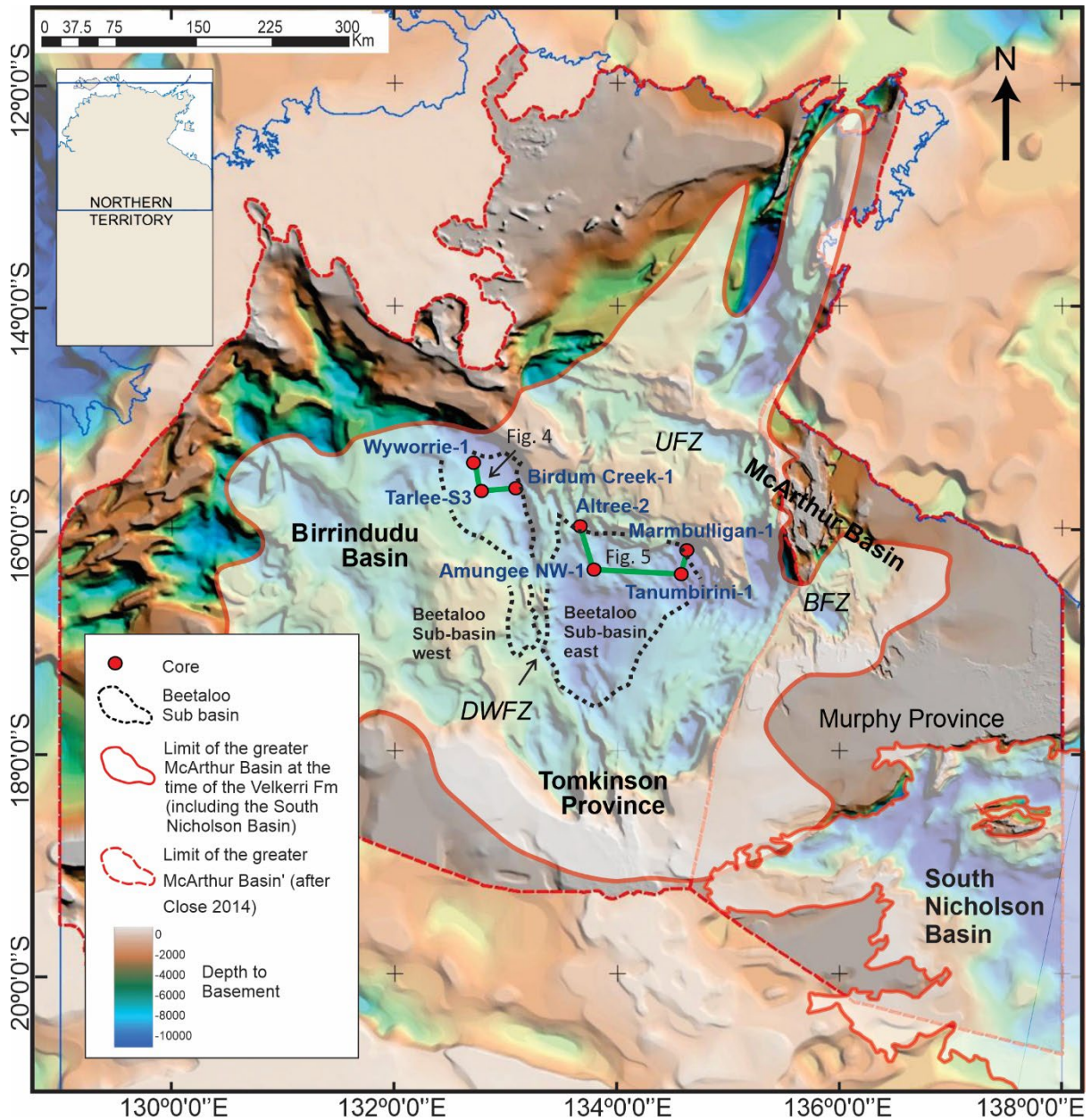


Figure 1. Regional map of the northern Northern Territory of Australia (inset shows location) showing the top-to-basement (SEEBASE™ basement surface image after Frogtech Geoscience, 2018), and location of drillholes used in this study. Green line locates the fence diagrams in Figs. 4 & 5. Limit of the Wilton Package after Close (2014) and extent of South Nicholson Basin after Raymond et al. (2018) and Jarrett et al. (2019b). BFZ = Batten Fault Zone, UFZ = Urupunga Fault Zone, DWFZ = Daly Waters Fault Zone.

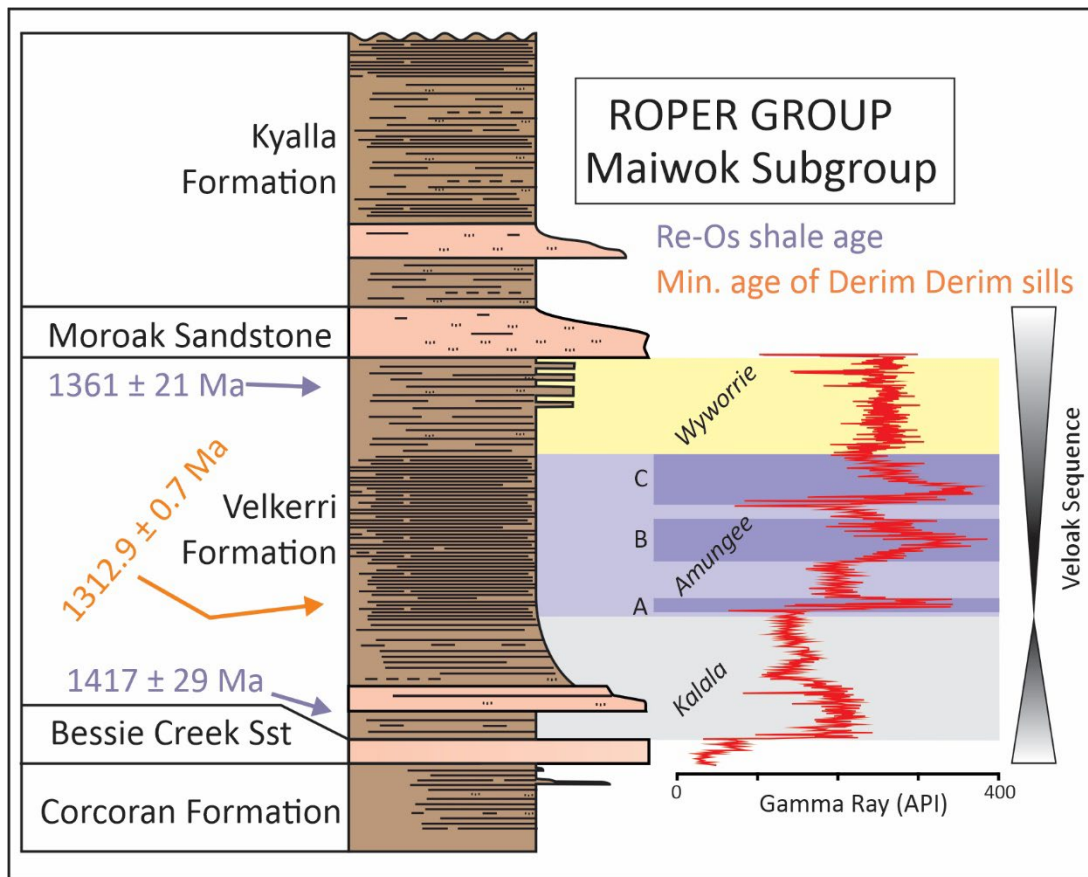


Figure 2. Stratigraphic succession of the upper Roper Group (Maiwok Subgroup). Composite gamma ray log from Munson & Revie (2018). 'A', 'B' and 'C' refer to three high organic carbon shales found in the Amungee Member. Kalala, Amungee and Wyworrie are members of the Velkerri Formation (Munson and Revie, 2018). Sst = sandstone. U–Pb baddeleyite age of crosscutting intrusion from Yang et al. (2020). Re–Os shale ages from Kendall et al. (2009). Triangles refer to sequence stratigraphic sequences of Abbott & Sweet (2000).

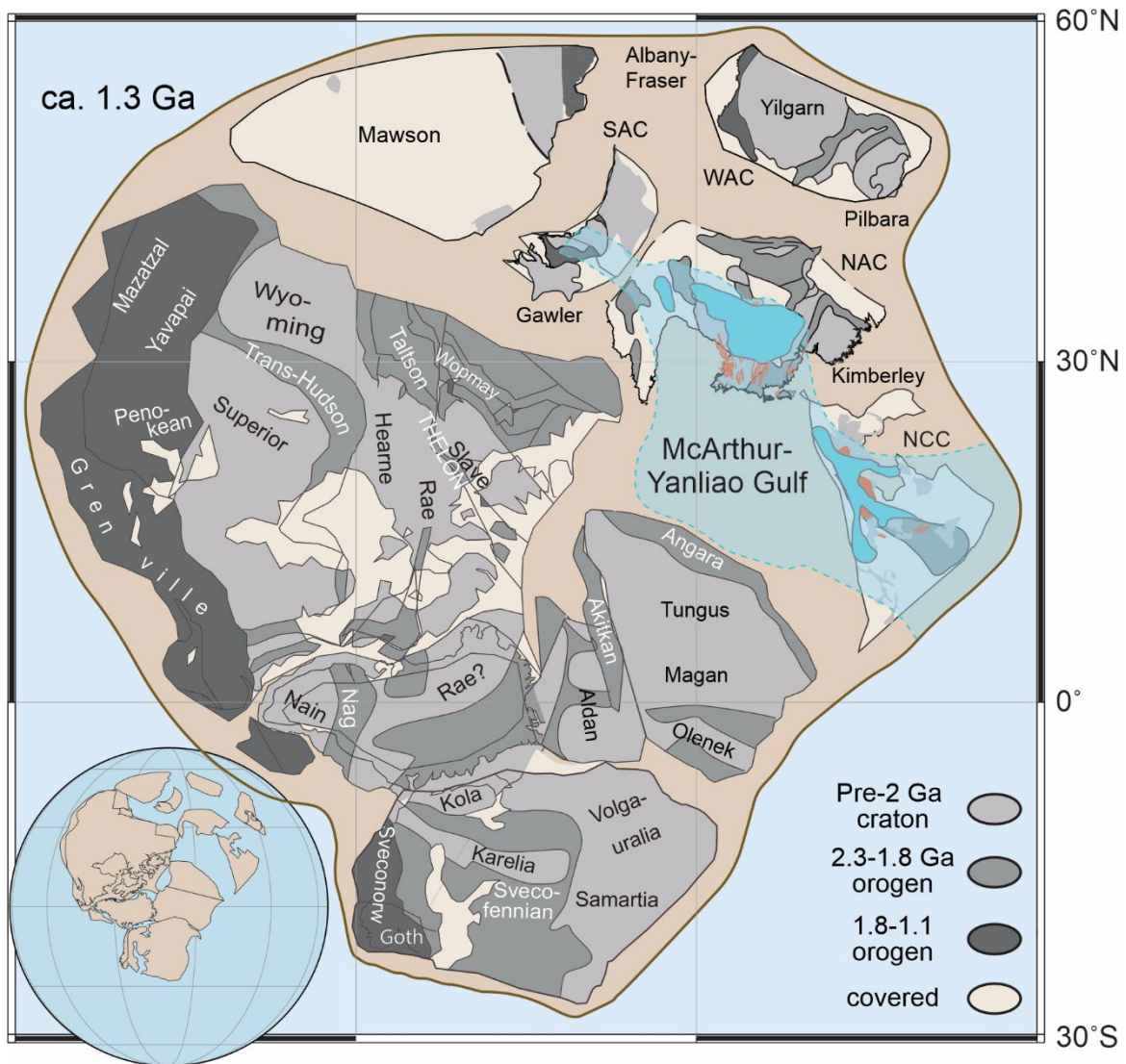


Figure 3. Continental reconstruction of Nuna/Columbia supercontinent at ca. 1.3 Ga, emphasizing the extent of the McArthur-Yanliao Gulf (light blue) and extent of extant basin distribution (medium blue). Red lines are dikes and sills associated with the ca. 1.3 Ga Derim Derim–Galiwinku–Yanliao Large Igneous Province. NCC = North China Craton, SAC = South Australian Craton, NAC = North Australian Craton, WAC = West Australian Craton. Map modified from Kirscher et al. (2018) and Collins et al. (2019).

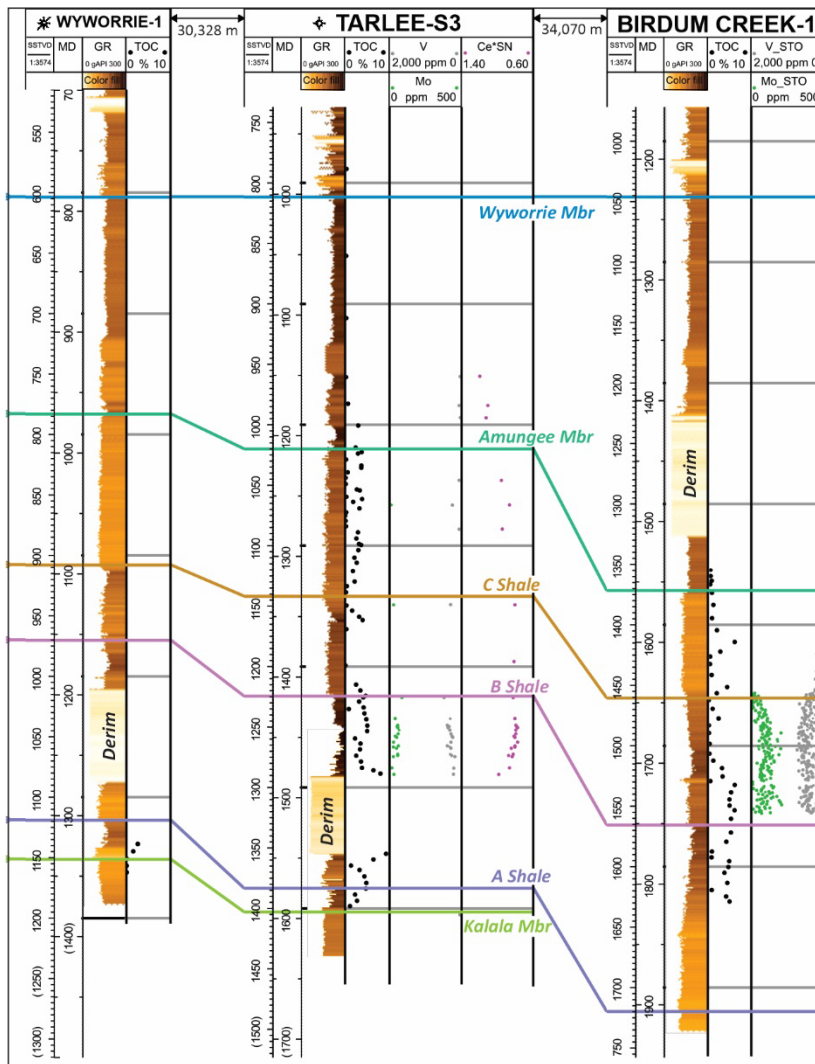


Figure 4. Fence diagram of the Velkerri Formation across the Beetaloo Sub-basin west (location on Fig. 1). Colored tie lines are the tops of the respective formations, Velkerri Formation Members (Mbr) and high-organic-content shale intervals (A, B, C shales) in the Amungee Member. SSTVD = Subsea True Vertical Depth, MD = Measured Depth, GR = Gamma Ray, TOC = Total Organic Carbon, CE*SN = Cerium anomaly. Derim = Derim Derim dolerite intrusion. V and Mo plotted in opposite senses in gray and green respectively.

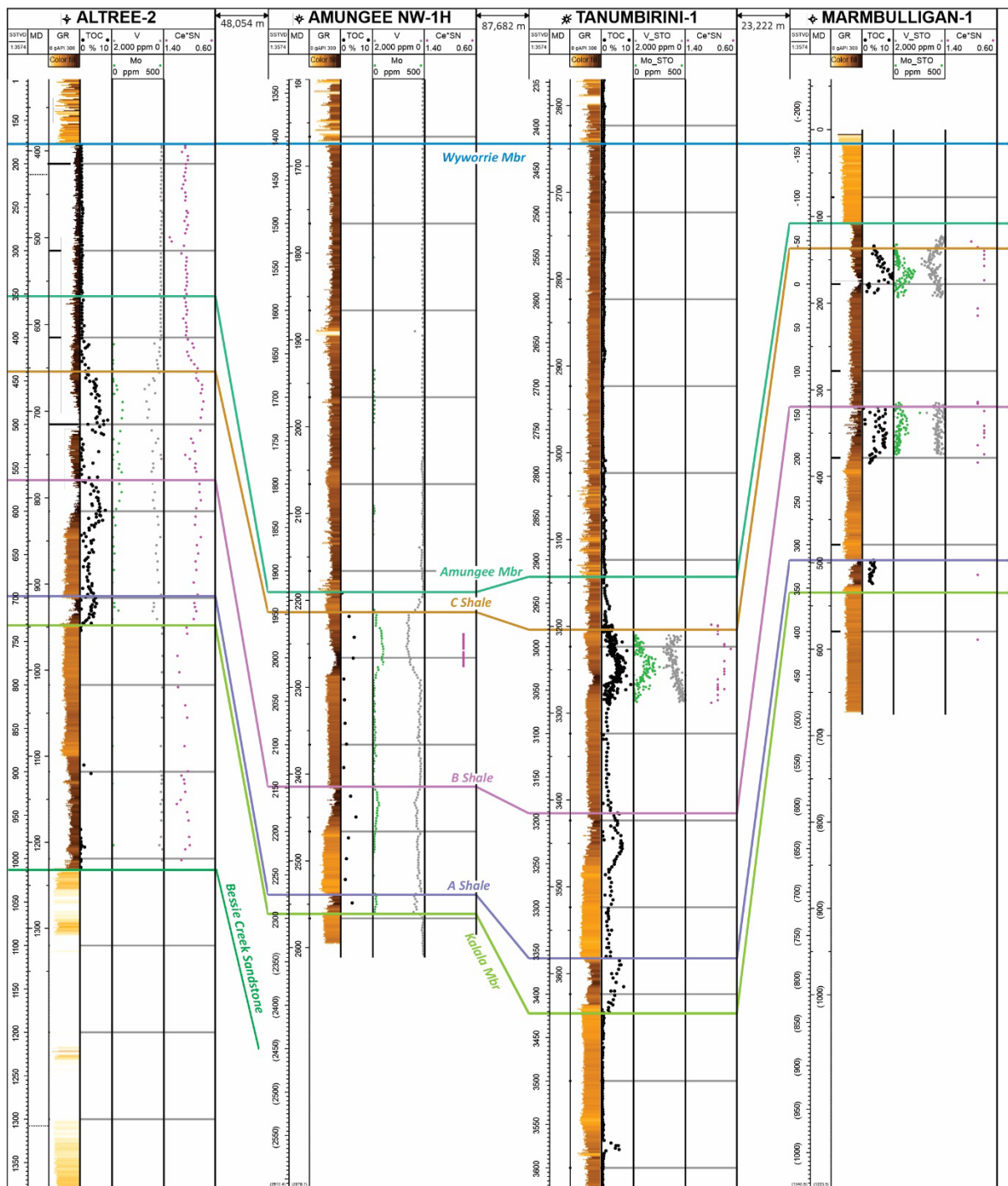


Figure 5. Fence diagram of the Velkerri Formation across the Beetaloo Sub-basin east (location on Fig. 1). Birdum Creek 1 (Fig. 4) and Atree 2 (Fig. 5) are separated by 76,141 m across the Daly Waters Fault Zone where the Velkerri Formation is still likely to be present (Williams, 2019). See Fig. 4 for key.

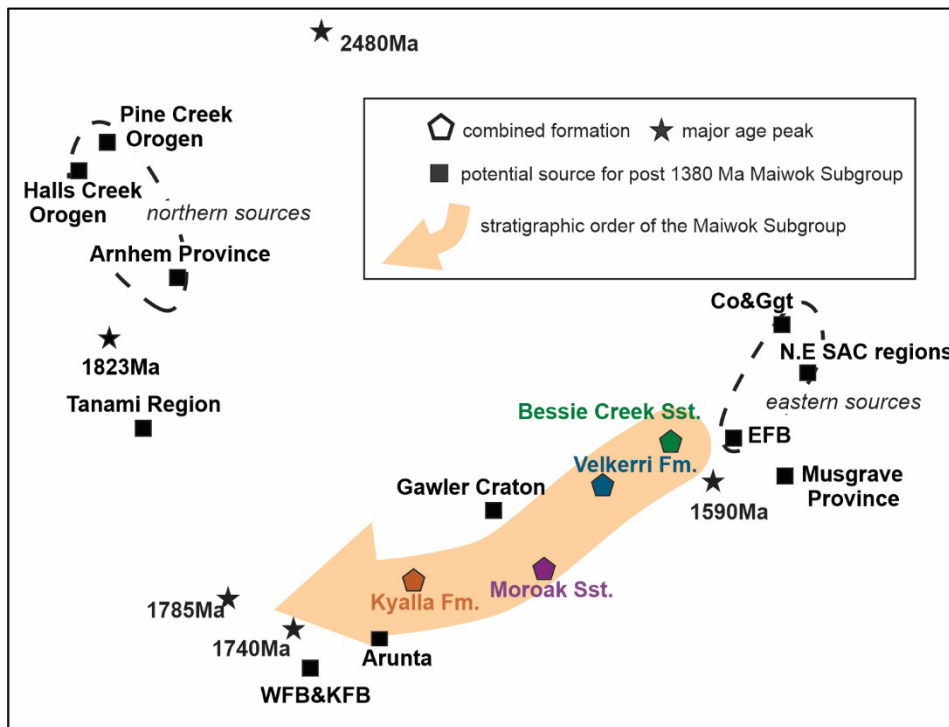


Figure 6. Multidimensional Scaling plot of Maiwok Subgroup detrital zircon U–Pb age data from Yang et al. (2018), Munson et al. (2018) and Fanning (2012). WFB –Western Fold Belt; KFB – Mary Kathleen Fold Belt; EFB – Eastern Fold Belt; Co & Ggt – Coen and Georgetown provinces. WFB, KFB and EFB are all in the Mount Isa Province. Stars represent synthetic data points generated to reflect main peaks within the Maiwok Supergroup data. Published data for potential source comparison are from igneous and sedimentary rocks older than 1380 Ma. Modified from Yang et al. (2018).

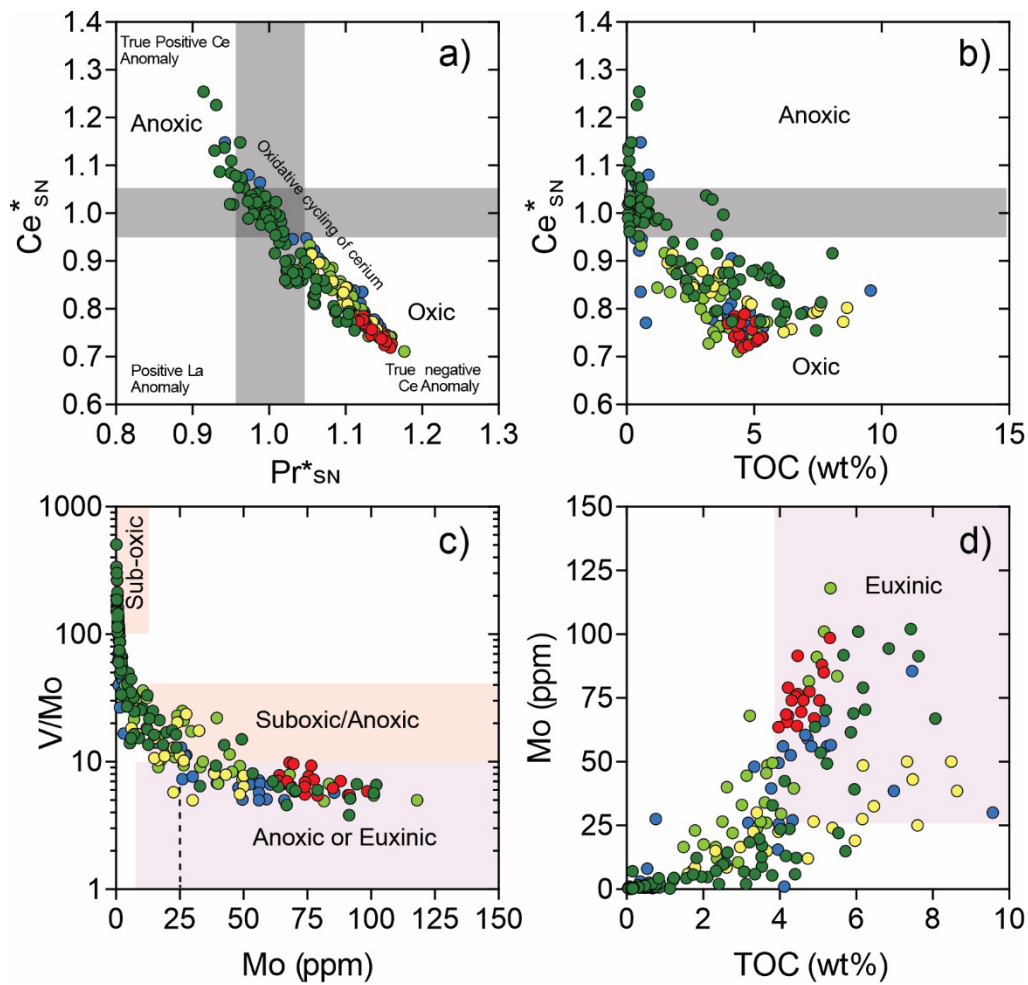


Figure 7. (A) Shale normalised Ce anomaly (Ce^*_{SN}) vs shale normalised Pr anomaly (Pr^*_{SN}). (B) Ce^*_{SN} vs total organic carbon (TOC). Elemental data normalised to the Post Archean Australian Shale (PAAS; Nance and Taylor, 1976). (C) V/Mo vs Mo with redox fields modified from Piper and Calvert (2009) (D) Mo vs TOC. Euxinic field after Cox et al. (2016). Dark green circles = Altree 2, red circles = Amungee NW-1H, blue circles = Tarlee S3, light green circles = Tanumbirini 1, yellow circles = Marmbulligan 1.

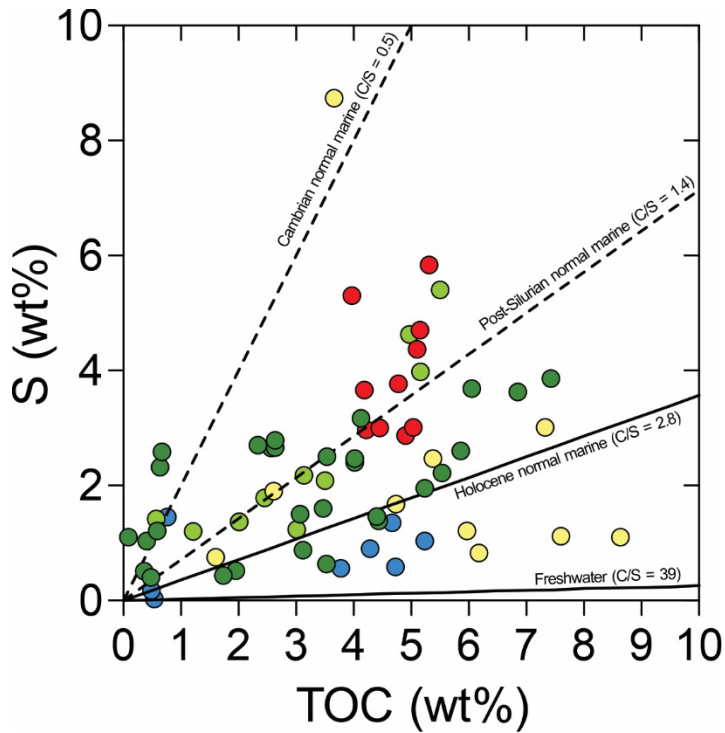


Figure 8. Sulfur-carbon systematics for the Velkerri Formation. Freshwater and Holocene normal marine C/S ratios are from Berner and Raiswell (1983). Post Silurian and Cambrian C/S ratios are from Lyons et al. (2000). Dark green circles = Atree 2, red circles = Amungee NW1, blue circles = Tarlee S3, light green circles = Tanumbirini 1, yellow circles = Marmbulligan 1.

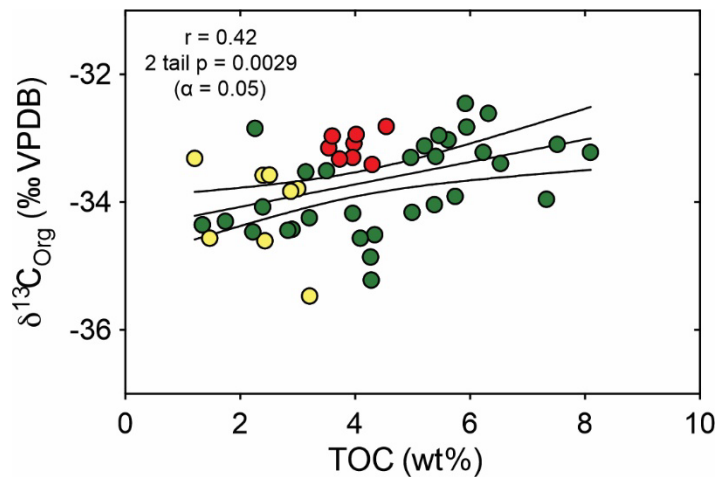


Figure 9. $\delta^{13}\text{C}$ vs TOC. Pearson correlation co-efficient is 0.4 and is statistically significant at alpha = 0.05 ($p = 0.0029$). Dark green circles = Atree 2, red circles = Amungee NW-1H, yellow circles = Marmbulligan 1.

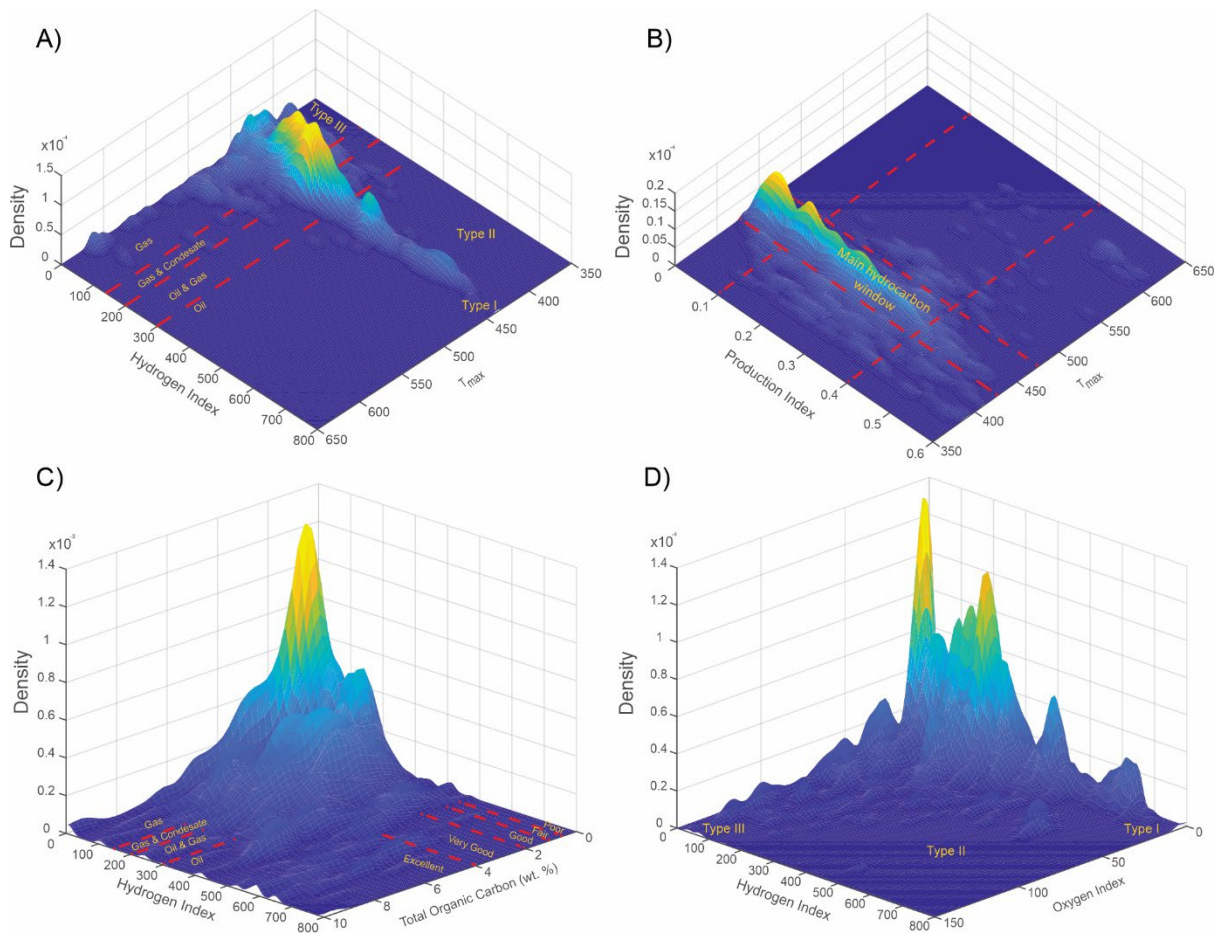


Figure 10. Kernel density estimates (KDE) for A) Hydrogen Index vs T_{max} B) Production Index vs. T_{max} C) Hydrogen Index vs Total Organic Carbon and D) Hydrogen Index vs Oxygen Index. KDE estimates are based on filtered pyrolysis data. Classification scheme is by Peters & Casa (1994).

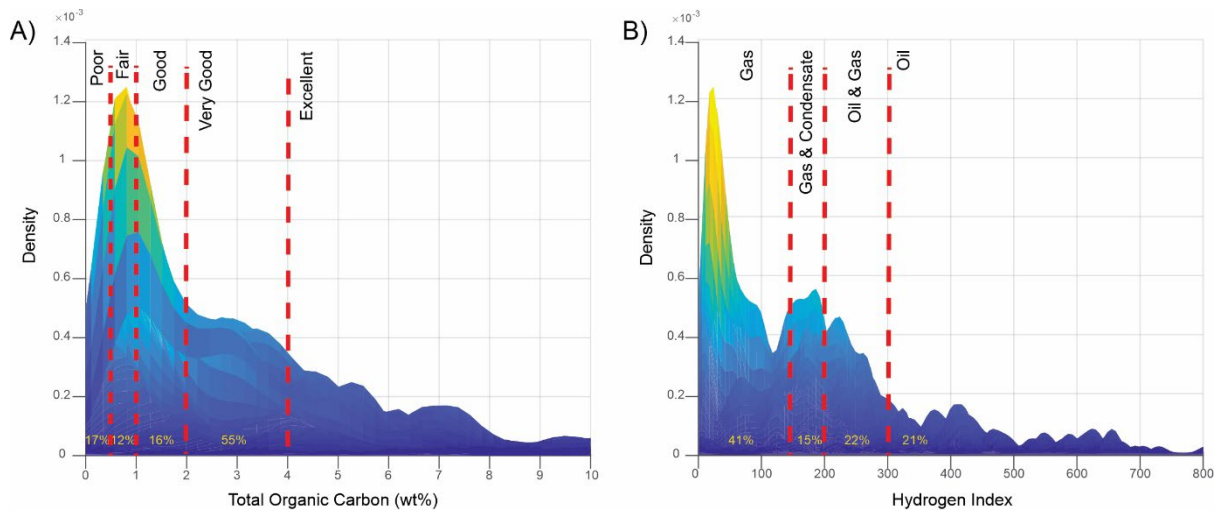


Figure 11. Kernel density estimates (KDE) for A) Total Organic Carbon and B) Hydrogen Index. Percentage values shown in yellow are area under curve calculations for each zone shown by the red dashed lines.

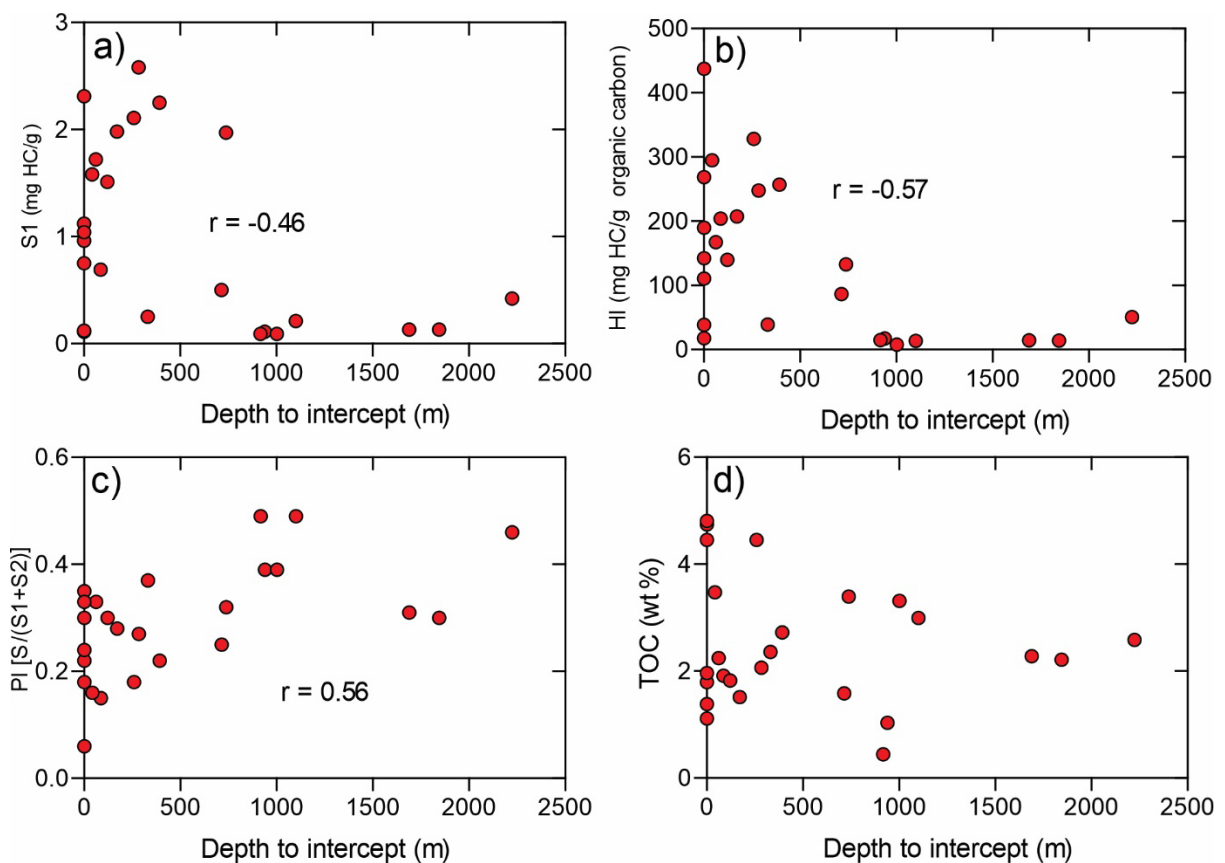


Figure 12. Cross-plot of average pyrolysis data versus depth to interception of the Velkerri Formation. Statistically significant correlations exist at the 95% confidence level for (A) S1 (B) Hydrogen Index (C) Production Index, but no statistically significant relationship exists for TOC. Statistical significance is based on a standard 2-tail test with alpha = 0.05 (pS1 = 0.02, pHI = 0.0035, pPI = 0.0035, pTOC = 0.51).

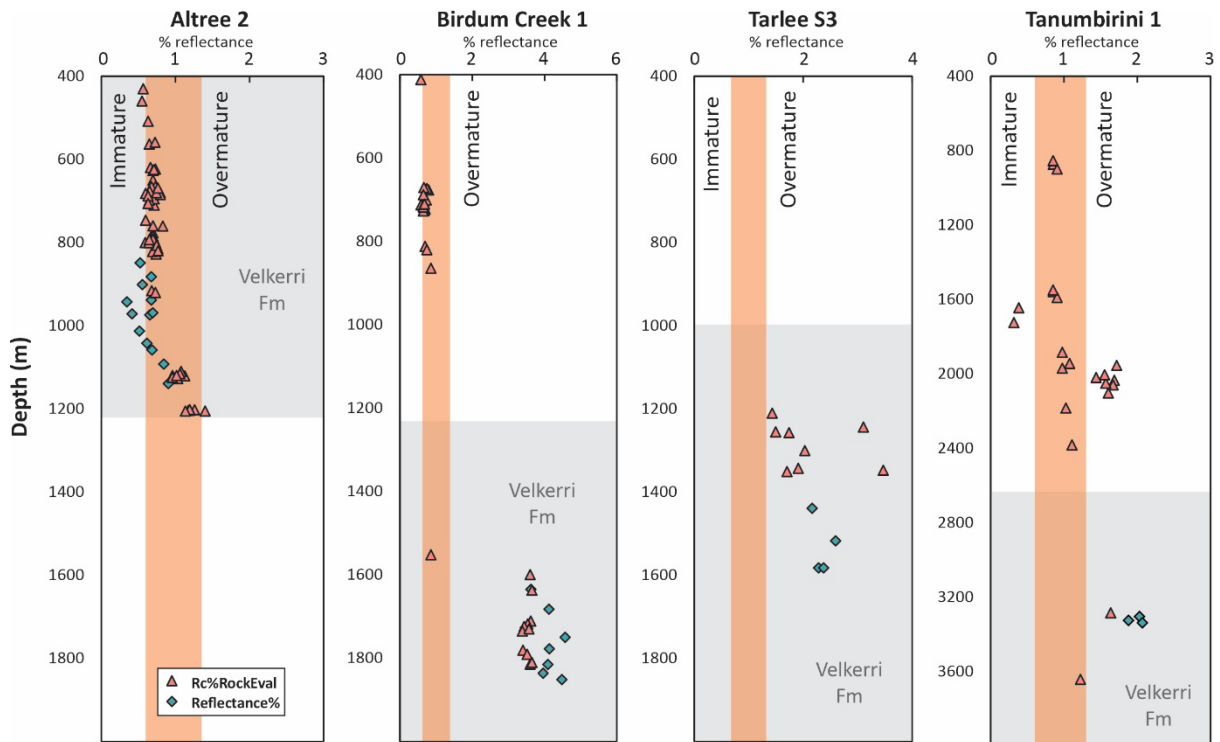


Figure 13. Organic maturity vs depth plots for four wells used in this study. Gray shaded areas are the depths of the Velkerri Formation in each hole. Peach color vertical column is a broad maturity window. Blue diamonds = solid bitumen reflectance values (from Revie & Normington, 2020). Pink triangles = calculated vitrinite-equivalent reflectance equivalents calculated from T_{max} using the Jarvie (2018) equation when $T_{max} > 400^{\circ}\text{C}$ and $< 580^{\circ}\text{C}$, and $S_2 > 0.5$.

Well	Year Drilled	Reservoir	Show Summary
Alexander 1	1987	Moroak Sandstone Velkerri Formation Bessie Creek Sandstone	Bitumen in vugs Oil bleeds and fluorescence Oil shows
Altree 2	1998	Velkerri Formation Amungee Member Bessie Creek Sandstone	Oil shows Oil and gas shows Oil staining
Amungee NW-1H	2015	Chambers River Formation Kyalla Formation Moroak Sandstone Middle Velkerri	Gas shows Gas shows Gas shows Gas shows and hydraulically fractured gas flows
Balmain 1	1992	Hayfield Mudstone Jamison Sandstone	Live oil show at 637m Oil bleeds
Beetaloo W-1	2016	Kyalla Formation	minor fluorescence at 1028 m and between 1045-1065m Gas shows
Borrowdale 2	1988	Bessie Creek Sandstone	Oil staining
Broadmere 1	1984	Velkerri Formation	Minor oil shows
Broughton 1	1988	Munyi Member Hodgson Sandstone Arnold Sandstone Limmen Sandstone	Solid bitumen at 93m Oil staining Oil staining Oil and gas shows
Burdo 1	1993	Moroak Sandstone	Gas show and minor oil fluorescence between 1014m-1030m
Chanin 1	1993	Bukalormi Sandstone	Gas shows
Elliott 1	1991	Kyalla Formation Moroak Sandstone	Oil shows Oil staining
Friendship 1	1988	Velkerri Formation	Gas shows
Jamison 1	1990	Jamison sandstone Bukalormi Sandstone Kyalla Formation	Drill stem test oil show Oil staining Oil bleeds and staining
Kalala S-1	2015	Kyalla Formation Velkerri Formation	Gas shows Gas shows
Lady Penrhyn 1	1987	Velkerri Formation Bessie Creek Sandstone	Oil staining Oil staining
Mason 1	1991	Chambers River Formation Bukalorkmi Formation	Oil and gas shows Oil and gas shows
McManus 1	1989	Velkerri Formation	Minor oil and gas shows
Prince of Wales 1	1987	Velkerri Formation	Fluorescence and bitumen in vugs
Ronald 1	1993	Moroak Sandstone	Minor gas shows
Scarborough 1	1987	Velkerri Formation	Oil shows, bitumen and oil in carbonate filled fractures
Sever 1	1990	Middle Velkerri	Minor gas shows
Shea 1	1991	Moroak Sandstone Velkerri Formation	Minor oil shows Oil shows
Shenandoah 1	2007	Hayfield Mudstone Jamison Sandstone Kyalla Formation	Gas show Hayfield Mudstone Gas show Jamison Sandstone Gas show Kyalla Formation
Shortland 1	1992	Chambers River Formation Bukalormi Sandstone	Fluorescence Fluorescence
Tanumbirini 1	2014	Velkerri Formation	Minor gas shows
Tarlee 1	2015	Amungee Member	Gas shows
Tarlee 2	2015	McMinn Kyalla Formation Amungee Member	Minor gas shows Minor gas shows Gas shows
Tarlee S3	2014	Velkerri Formation	Oil and gas shows
Urapunga 4	1985	Velkerri Formation	Oil bleed
Walton 2	1989	Moroak Sandstone Velkerri Formation	Fluorescence Oil and gas shows

Table 1. Roper Group hydrocarbon show summary. All data compiled from Well Completion Reports, which are available from: <https://geoscience.nt.gov.au/gemis/>.

Well	Latitude	Longitude	T _{max}		S1		S2		S3		PI		HI		OI		TOC		Number of Samples
			Mean	95% CI	Mean	95% CI	Mean	95% CI	Mean	95% CI	Mean	95% CI	Mean	95% CI	Mean	95% CI	Mean	95% CI	
Alexander 1	-15.17	134.86	412.25	26.27	1.72	0.77	4.43	2.34	0.46	0.2	0.33	0.07	167.23	43.96	66.76	41.2	2.24	0.96	70
Altrec2	-15.92	133.79	437.49	4.82	2.25	0.39	10.99	2.93	0.44	0.11	0.22	0.04	257.03	44.55	19.34	5.9	2.72	0.57	260
Amungee NW-1H	-16.35	133.88	360.53	19.74	0.13	0.09	0.28	0.17	0.6	0.18	0.31	0.11	14.34	8.32	41.46	19.09	2.28	1.34	15
Birdum Creek	-15.63	133.14	486.66	76.98	0.21	0.1	0.3	0.43	0.15	0.07	0.49	0.05	13.4	20.86	8.55	5.87	2.99	1.4	35
Borrowdale 2	-15.12	133.82	426.45	15.06	1.12	0.4	6.1	2.76	0.31	0.13	0.22	0.05	142.19	38.56	24.78	8.62	4.45	1.94	110
Friendship 1	-14.88	133.91	437.84	33.96	0.36	0.35	0.96	0.9	0.31	0.19	0.29	0.05	61.52	30.18	43.9	13.34	1.61	1.23	30
Golden Grove	-14.84	134.36	460.14	34.83	0.15	0.23	1.46	3.27	0.05	0.05	0.18	0.06	54.32	61.4	4.08	1.61	1.44	1.79	14
Kalala S1	-16.29	133.61	358.02	4.55	0.13	0.05	0.28	0.1	0.66	0.1	0.3	0.05	13.77	3.05	46	13.73	2.21	0.95	35
Lady Penrhyn 1	-15.08	134	441.08	14.01	1.98	1.13	5.23	2.94	0.31	0.13	0.28	0.07	207.15	41.78	16.95	4.39	1.51	0.88	51
Lady Penrhyn 2	-15.08	134	442.48	2.31	0.69	0.18	4.6	1.48	0.27	0.09	0.15	0.03	204.13	21.76	25.48	8.56	1.91	0.6	99
Lawrence 1	-14.98	133.89	475.84	38.77	0.11	0.13	0.19	0.2	0.11	0.06	0.35	0.1	38.71	31.09	37.51	24.2	1.11	1.51	12
McManus 1	-15.92	133.63	437.1	10.35	1.97	0.48	4.48	1.26	0.38	0.1	0.32	0.05	132.78	35.46	17.77	7.1	3.39	0.69	167
Prince of Wales 1	-14.76	133.95	414.66	37.54	0.96	0.59	3.01	1.9	0.45	0.33	0.3	0.11	110.59	46.31	60.18	49.58	1.79	0.94	50
Scarborough 1	-15.18	134.8	437.7	5.18	1.51	0.61	3.57	1.68	0.42	0.24	0.3	0.04	139.61	32.99	30.67	17.82	1.82	0.71	81
Sever 1	-15.25	132.84	394.75	34.33	0.25	0.16	0.5	0.3	0.34	0.3	0.37	0.08	39.1	25.3	30.15	10.33	2.36	1.21	121
Shea 1	-15.07	133.76	434.33	4.82	2.58	0.84	7.51	2.64	0.41	0.15	0.27	0.05	247.55	44.99	22.54	6.52	2.06	0.77	101
Shenandoah 1	-16.62	133.58	381.45	24.94	0.11	0.07	0.16	0.08	0.35	0.1	0.39	0.09	17.28	6.15	43.42	6.98	1.03	0.23	128
Supply 1	-15.21	134.77	430.21	12.73	0.75	0.53	3.16	3.63	0.38	0.16	0.24	0.11	189.63	69.88	45.98	30.71	1.38	1.05	15
Tanumbirini 1	-16.4	134.7	391.14	31.81	0.12	0.03	0.26	0.09	0.55	0.16	0.33	0.07	17.53	6.57	39.88	8.97	1.96	0.71	47
Tarlee 1	-15.95	132.84	503.58	59.24	0.09	0.07	0.09	0.07	0.23	0.15	0.49	0.21	14.9	5.72	42.01	18.03	0.44	0.22	12
Tarlee 2	-15.89	132.68	430.58	38.67	0.5	0.47	1.29	1.15	0.5	0.11	0.25	0.08	86.47	50.26	61.45	19.87	1.58	1.32	19
Tarlee 3	-15.63	132.83	438.1	43.13	0.09	0.04	0.14	0.05	0.35	0.2	0.39	0.05	7.59	3.42	28.11	16.83	3.31	1.16	68
Walton 1	-15.93	133.67	434.86	11.31	2.11	0.58	21.55	8.41	1.07	0.59	0.18	0.04	328.21	80.58	29.68	11.39	4.45	1.39	112
Urapunga-3	-14.65	133.75	435.18	5.71	2.31	0.29	12.98	2.79	0.15	0.02	0.18	0.04	268.36	32.13	3.33	0.17	4.74	0.66	20
Urapunga-4	-14.71	134.29	439.13	2.11	1.58	0.45	12.44	5.57	0.12	0.01	0.16	0.03	294.84	39.07	6.77	1.33	3.47	1.24	22
Marrbulligan 1	-16.2	134.77	438.35	1.83	1.04	0.18	22.92	5.84	0.19	0.02	0.06	0.01	437.34	56.96	5.21	4.27	4.81	0.84	100
All - Unfiltered			428.79	2.39	1.17	0.06	6.92	0.53	0.42	0.03	0.26	0.01	167.12	7.73	30.16	2.73	2.65	0.11	1861
All - Filtered			438.37	1.6	1.43	0.06	8.56	0.62	0.43	0.03	0.23	0.01	200.68	8.44	23.73	1.66	2.81	0.12	1442

All values calculated using Monte Carlo Bootstrap Simulation.

Table 2. Bootstrapped pyrolysis data for unfiltered and filtered datasets along with data for individual wells. Methods for calculations can be found in the Supplementary Information.